I.J. Image, Graphics and Signal Processing, **2023, 5, 39-59**
Published Online on October 8, 2023 by MECS Press (http://www.mecs-press.org/)
DOI: 10.5815/ijigsp.2023.05.04

A Statistical Approach for Investigation and Comparison of Fatigue and Drowsiness based on Complexity Parameters of EOGs

Ashis Kumar Das*
Department of Electrical Engineering, National Institute of Technology, Durgapur, 713209, India
Faculty of Technology, Uttar Banga Krishi Viswavidyalaya, Cooch Behar, 736165, India
E-mail: ashiskd11@gmail.com, ashis@ubkv.ac.in
ORCID iD: https://orcid.org/ 0000-0002-0013-7176
*Corresponding Author

Prashant Kumar
Department of Electrical Engineering, National Institute of Technology, Durgapur, 713209, India
E-mail: raja.prashant89@gmail.com
ORCID iD: https://orcid.org/ 0000-0003-2492-1202

Suman Halder
Department of Electrical Engineering, National Institute of Technology, Durgapur, 713209, India
E-mail: shalder.ee@nitdgp.ac.in
ORCID iD: https://orcid.org/ 0000-0003-0219-9562

Santanu Metia
Faculty of Engineering and Information Technology, University of Technology Sydney, Sydney, NSW 2007, Australia
E-mail: Santanu.Metia@uts.edu.au
ORCID iD: https://orcid.org/ 0000-0002-5676-1146

Received: 26 December 2022; Revised: 25 February 2023; Accepted: 11 May 2023; Published: 08 October 2023

Abstract: The primary factors contributing to road accidents are drowsiness and fatigue. Additionally, it diminishes productivity within work environments and elevates the likelihood of accidents. The analysis of bio-signals is crucial in the examination of various physical conditions and the physiological state of an individual. Various biological signals were utilized to identify the presence of fatigue and drowsiness that is associated with fatigue. Various physiological signals were employed to identify driver or operator fatigue and drowsiness. Out of all these non-invasive signals, electrooculogram (EOG) exhibits well-accepted outcomes for detecting drowsiness and fatigue. By employing an EOG-based study, the real-time monitoring of the muscle and mental fatigue of the human subject can be done when they are engaging in their everyday activities. The present studies sought to employ a statistical analysis of electrooculograms (EOGs) to ascertain the stress levels of participants and provide insight into their state of fatigue and drowsiness. Two different experimental studies were performed with 120 and 80 healthy male and female research scholars of National Institute of Technology Durgapur, India. EOGs were recorded by the Biopac MP 45 data acquisition system at two and three different sessions of a day with huge cognitive tasks in between. Several entropies are evaluated from the time domain and frequency domain. The others complexity parameters are also incorporated to enrich the results of the experimental processes. An inferential statistical analysis based on the parametric t-test and non-parametric Wilcoxon test for study-I was considered to compare the stress levels between morning and evening sessions. Similarly, in study-II, the parametric ANOVA test and non-parametric Friedman test were carried out to monitor stress level in three different sessions of a day. The Tukey-Kramer post-hoc test is also undertaken to compare the outcomes among three different sessions and find the statistical differences based on a 5% significance level. Most complexity parameters show excellent results and clear differences in fatigue states for both the experiments and these analyses indicates the presence of onset fatigue among the subjects under consideration.

Index Terms: Electrooculogram (EOG), Fatigue, Stress, Visual cue, Entropy, Complexity parameter, Statistical analysis.

1. Introduction

As per the 2018 WHO Global status report on road safety, an estimated 1.35 million people lose their lives in traffic-related accidents each year. The greatest cause of death for those aged 5 to 29 is increasingly traffic-related injuries. This indicates that 3700 people pass away on the planet's highways every day. According to the WHO, millions of individuals suffer injuries in auto accidents each year. These wounds may be serious or not. These factors have led to the emergence of studies on road safety, one of which is the detection of driver drowsiness. Pedestrians, bikers, and motorcyclists, particularly those who reside in developing nations, are disproportionately burdened [1]. A driver's mental state during driving has a substantial effect on driving behaviors and is a major threat to road safety [2]. Driving when fatigued is a harmful habit that is seriously compromising transportation safety [3]. Drowsiness is associated with a range of lifestyle and environmental factors. These factors include but are not limited to, length of sleep, quality of sleep, the circadian cycle, age, level of fitness, consumption of alcohol, noise levels at work environments, vehicle temperature, driving schedule, as well as road-related aspects such as monotonous driving conditions, vehicle density, as well as lane density [4]. The driving during nighttime hours is associated with an increased risk factor of approximately three to six times when compared to driving during daylight hours. This is due to the heightened likelihood of individuals experiencing drowsiness and impaired vision [5]. In comparison to other contextual variables, research has demonstrated that monotonous driving can have a notable adverse effect on the driver's cognitive stimulation, leading to rapid onset of drowsiness [6]. The failure of drivers to evaluate their level of drowsiness frequently results in fatalities. Drivers' situational awareness and reaction time are reduced when they fall asleep behind the wheel [7]. Furthermore, drowsiness weakens the driver's decision-making ability. Drowsiness monitoring systems at the wheel are designed to prevent drowsiness-related traffic fatalities, that are why installing these systems in vehicles is critical nowadays. Drowsiness has been categorized into three stages in the study [8], based on EEG band power, blink characteristics, and eye movement patterns. The initial stage of drowsiness, according to this study, is lower vigilance, which is indicated by increased EEG theta band power and decreased ocular (eye ball and eyelid) movements. The second stage, sleep tendency, is characterized by longer lid reopening and higher blink duration. Enhanced blink frequency characterizes the final phase in which a driver nearly loses the ability to respond to traffic situations. To investigate the detection of drowsiness, a variety of methods are used, such as surveilling vehicular measurements, behavioral measurements of drivers, as well as driver physiological measurements. Most of the time, police logs are used to come up with vehicle-based measures. Included in these statistics are the speed of driver, displacement of lane, movements of steering wheel, and different patterns of braking. Using a camera, behavioral measures are acquired from the driver's face/eye movement. Analyzing data such as heart rate, electrocardiogram (ECG) [9], electroencephalogram (EEG) [10, 11], electromyogram (EMG) [12, 13], and electrooculogram (EOG) [14] that might be utilized as markers of driver drowsiness is the basis for physiological measures. Physiological approaches are based on the concept of detecting the initiation of driver drowsiness by using physiological signals that change in the initial phases of drowsiness [15]. Early diagnosis of drowsiness may provide the system with additional time to inform a drowsy driver in time to prevent a traffic collision. The capacity to identify human fatigue with related drowsiness with a low rate of error has inspired a number of researchers to conduct several investigations using several electrophysiological signals of a human body, including the electrocardiogram (ECG) [16], electrooculogram (EOG), electroencephalogram (EEG) [17].

Short-term indicators in the workplace have been found to result in decreased performance, productivity, and work quality, as well as heightened occurrences of workplace accidents and human errors [18]. According to research, employees who experience fatigue are more likely to report instances of lost productivity time due to health issues, compared to their non-fatigued counterparts. This difference is observed to be more than two-fold [19].

Existing approaches for evaluating driver and operator fatigue are limited in some ways. Although subjective assessment is extensively employed, it has inherent flaws, such as the expectancy bias, and can disrupt normal work, making it inappropriate for continuous real-time assessment of mental fatigue. Furthermore, it is unreasonable to continuously require drivers/operators to disclose their condition [20]. Lighting has a substantial impact on the vision-based monitoring strategy. 30% of the performance could be lost due to daylight reflection and glass reflection [21]. Present vision-based monitoring techniques are effective for frontal faces, but extreme head position will lead to inaccurate monitoring results [22]. Due to its low power consumption, low cost, commensurate speed, and lack of impact on the driver's field of view, EOG is a promising fatigue monitoring technique on the basis of physiological signals. EOG can also track eye movements in great detail.

This study evaluates the fatigue and associated drowsiness experienced by individuals who engage in sedentary work or hold professional occupations. This paper assesses the fatigue and accompanying drowsiness of sedentary employees and professionals during experimental research. It describes a method for assessing statistical variations in the time domain, frequency domain entropies, and other complexity factors of EOG signals in order to investigate fatigue of volunteer participants. In a session-by-session analysis, the statistical technique experimentally assessed fatigue and drowsiness. All the statistical test were performed at 5% significance level. Performing statistical tests at a 5% significance level means that the probability of rejecting the null hypothesis when it is actually true (known as a Type I error) is limited to 5% or less.

The remainder of the paper is organized as follows. Material and proposed methodologies are given in section 2. Section 3 presents the experimental results and discussion. Section 4 discusses the experimental limitations. In section 5, the paper is concluded.

2. Material and Methodologies

The obtained time series subsequently denoised to remove interference from power lines, respiration, and muscle movement that caused low- and high-frequency artifacts. Cue patterns were investigated in four different movements: RCW (clockwise rectangular motion), RAC (counterclockwise rectangular motion), TCW (clockwise triangular motion), and TAC (counterclockwise triangular motion). After pre-processing the data, all of the complexity parameters were assessed, and inferential statistical analysis was performed on the complexity parameters to verify the hypothesis about detecting fatigue and, consequently, drowsiness in the willing participants.

2.1. Participants

In this experimental process two datasets were used to emphasize two different studies. First dataset of 120 healthy participants has been incorporated and out of that 72 were males with mean age of 27.61 (95% CI: 26.73-28.49) and 48 were female with mean age of 24.96 (95% CI: 24.29-25.63). In the other study, a dataset of 80 participants was used, out of that 47 are males with mean age of 27.11 (95% CI: 26.12-28.10) and 33 are female with mean age of 25.36 (95% CI: 24.61-26.12). The number of participants is kept as much as possible to produce reliable outcome of this biomedical study [23]. The volunteer participants are basically the research scholars of the National Institute of Technology Durgapur, India. The data samples were taken on faith of good mental and physical health of the subjects and steps were taken to minimize the circadian effect. Table 1 and Table 2 show the vital data of the participants.

Table 1. The vital data of the participants for study-I in term of Mean ± Sd with 95% CI.

Parameters	Male (N=72)		Female (N=48)	
	Mean ± SD	95% CI	Mean ± SD	95% CI
Age (years)	27.61 ± 3.74	26.73-28.49	24.96 ± 2.30	24.29-25.63
Height (cm)	166.09 ± 6.07	164.66-167.51	157.07 ± 4.39	155.80-158.34
Weight (Kg)	71.61 ± 8.03	69.72-73.50	60.25 ± 4.57	58.92-61.58
BMI (Kg/m2)	25.93 ± 2.50	25.34-26.52	24.40 ± 1.05	24.09-24.70
SBP (mmHg)	120.43 ± 5.30	119.19-121.68	116.44 ± 4.01	115.27-117.60
DBP (mmHg)	80.90 ± 2.86	80.23-81.57	79.83 ± 2.22	79.22-80.45

Table 2. The vital data of the participants for study-II in term of Mean ± Sd with 95% CI.

Parameters	Male (N=47)		Female (N=33)	
	Mean ± SD	95% CI	Mean ± SD	95% CI
Age (years)	27.11 ± 3.37	26.12-28.10	25.36 ± 2.13	24.61-26.12
Height (cm)	165.58 ± 6.18	163.77-167.40	156.65 ± 3.96	155.24-158.05
Weight (Kg)	70.83 ± 8.25	68.41-73.25	59.85 ± 4.02	58.42-61.28
BMI (Kg/m2)	25.79 ± 2.48	25.07-26.52	24.37 ± 0.91	24.05-24.70
SBP (mmHg)	120.92 ± 5.16	119.40-122.43	116.42 ± 4.12	114.96-117.89
DBP (mmHg)	81.02 ± 2.95	80.15-81.88	79.24 ± 2.18	78.47-80.01

2.2. Experimental paradigm

Under the broad version of this experimental process, here two studies are performed. In study-I, the EOG data of participants are recorded for 14 min 02 sec twice a day. One session is at morning at around 8 am and another session is at evening at around 8 pm. In study-II, beside the morning and evening, EOG data is also collected at afternoon session at around 2 pm. The participants are asked to engage in intense cognitive activity between data collection for study-I and as well as for study-II. Fig. 1 depicts the outline of the experimental methodology. Before data collection, the experimental protocol was explicitly communicated to participants and written consent was obtained from them. The Declaration of Helsinki Ethical Principles was followed in the entire experimental study. The Institutional Ethical Committee (IEC) of National Institute of Technology Durgapur, India has granted approval for the study and the collecting of physiological data. All participants were instructed to desist from alcohol consumption the night before and from caffeine, nicotine, and other amphetamines two hours prior to data collection. During acquisition, they are also instructed to remain calm, breathe regularly, inhibit voluntary eye blinking, and avoid body movement and speech. All the data were recorded in the Biomedical engineering laboratory at ambient temperature and with a minimum interference of radio waves.

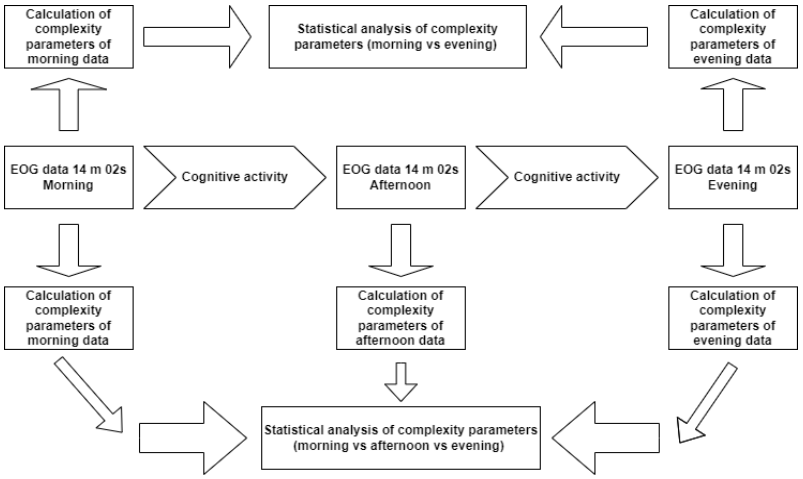

Fig. 1. Outline of experimental methodology.

2.3 Visual cue

In this experimental investigation, a VR (virtual reality) -displayed video [24] of a visual cue was used to initiate and control eye movement in a predetermined direction and speed. Participants were instructed to adhere to the protocol [25, 26]. Four patterns were incorporated into the cue movement. Various eye movements like gazing, smooth pursuit, and saccades, were incorporated into the process of monitoring the movement of a cue in a predefined direction so that the reflection of those movements could be acquired effectively. There were four distinct cue movement patterns (each lasting 16 seconds), and a 10-second gazing period was inserted between each pair of patterns to make clear differences between two patterns. The cue movement pattern is depicted as

Gazing → RCW → Gazing → RCW → Gazing → RCW → Gazing → RCW → Gazing → RCW → Gazing → RCW → Gazing → RCW → Gazing → RAC → Gazing → RAC → Gazing→ RAC → Gazing → RAC → Gazing → RAC → Gazing→ RAC → Gazing → RAC → Gazing → RAC → Gazing → TCW → Gazing → TCW → Gazing → TCW → Gazing → TCW → Gazing → TCW → Gazing → TCW → Gazing → TCW → Gazing → TCW → Gazing → TAC → Gazing → TAC → Gazing → TAC → Gazing → TAC → Gazing → TAC → Gazing → TAC → Gazing → TAC → Gazing → TAC → Gazing (RCW: Clockwise rectangular, RAC: Counter clockwise rectangular, TCW: Clockwise triangular, TCW: Counter clockwise triangular)

2.4 Data acquisition and pre-processing

The EOGs of the participants were acquired at different time of throughout the day by a data acquisition device MP 45 made by BIOPAC Systems, Inc. MP 45 is a two channel 16-bit computer interfaceable data acquisition system. It is a CE marked device which complies with IEC 60601-1 (technical standards for the safety and effectiveness of medical electrical equipment) and IEC 60601-1-2 (Electromagnetic Compatibility of Medical Devices). Electrode lead wire (SS2LB) was connected as input device to MP 45 for this study. Medico electrodes Msglt_05 (disposable) were affixed with lead wire SS2LB connected to the surfaces of skin at specific facial locations to acquire electrical signal. The EOGs were recorded at 2 kHz sampling frequency. The experimental setup, electrode positioning layout and MP 45 data acquisition system are depicted in Fig. 2, Fig. 3 and Fig. 4 respectively. The cornea movements and blinks were acquired by horizontal channel and the vertical channel of MP 45 respectively and were recorded at BIOPAC student Lab 4.1 software which was installed in computer and associated with MP 45 hardware system. The electrooculogram signal has a frequency range of 0 to 50 Hz. One of the essential phases in pre-processing EOG signal is to removing noise from the signal. This was done by using a suitable noise filter that removes and reduces noise components like baseline from different sources corresponding to breathing, muscle movement, and power line frequency interference (PLI) from cables that carry the electrooculogram signal. It makes the signal-to-noise ratio (SNR) better for further processing. Thus, raw electrooculogram signal was filtered before it was used for further analysis and processing.

Fig. 2. Experimental setup for EOG Data acquisition by BIOPAC MP45.

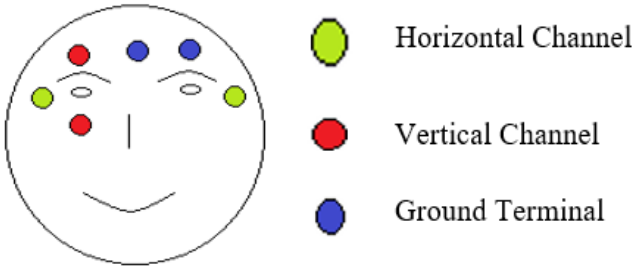

Fig.3. MP 45 (BIOPAC) electrode positioning.

Fig. 4. MP 45 (BIOPAC) Data acquisition system.

2.5 Complexity parameters

The complexity analysis of acquired EOGs were evaluated to measure fatigue and drowsiness of the participants. The overall EOG signals for the morning and evening horizontal movement activity periods in study-I was segregated into four distinct parts and examined individually. Eight clockwise rectangular (RCW), eight counterclockwise rectangular (RAC), eight clockwise triangular (TCW), and eight counterclockwise triangular (TAC) cue movements each of 128 sec durations were extracted in part-1 through part-4 to separate out the four different patterns effectively. In study-II, EOG signals from the horizontal movement activity periods in the morning, afternoon, and evening were taken into consideration individually to compose three different templates, each lasting for 512 seconds and without taking the gazing period into account. In the process of analyzing the dynamic properties of signals, entropy is one of the nonlinear notions that is utilized the majority of the time [27]. This is an index of complexity analysis that measures the level of system confusion inside a time series. These techniques take into account both the complexity and the unpredictable nature of the signal. Irregular signals are more complex than regular ones due of their greater unpredictable nature. According to some academics, these methods can be used to evaluate time series in the time domain or frequency domain. Entropy primarily reflects changes in time in the temporal domain, and these studies are continually getting better. There are many other ways to measure complexity besides the entropy method. The different complexity analysis was done with the horizontal EOG signal.

2.5.1 Approximate entropy

Appropriate entropy [28, 29, 30] (ApEn) is a measure of the overall features of the response signal in terms of the signal's complexity. It works well for separating the signal from random signals and is practical for small datasets. To calculate ApEn, m and r, two input parameters, must be fixed. m is the length of the runs being compared, and r acts

like a filter. For N data points $u\{i\}$ creates vector array $x(1)$ to $x(N-m+1)$ expressed by $x(i)=[u(i),.....,u(i+m-1)]$. These vectors indicate *m* successive *u* values, starting at the i^{th} position. The greatest difference between the scalar components of two vectors *x(i)* and *x(j)* are the distance between them, denoted as $d[x(i),x(j)]$. Employing the array $x(1),x(2),.....,x(N-m+1)$ to construct for every $i \le N-m+1$, $C_i^m(r)=(\text{number of } j \le N\text{ - }m+1 \text{ such that } d[x(i),x(j) \le r])/(n-M+1)$. The $C_i^m(r)$ measure the regularity or frequency of patterns comparable to a given pattern of window length m within a tolerance of r. By defining $\phi^m(r)=(N-m+1)^{-1}\sum_{i=1}^{N-m+1}\ln C_i^m(r)$, where ln be the natural logarithm and for given values of *m*, *r* and *n*, approximate entropy is given as

$$ApEn(m,r,N)=\phi^m(r)-\phi^{m+1}(r) \tag{1}$$

2.5.2 Sample entropy

Sample entropy [31] (SampEn) is a different approach for estimating entropy in real-world data. It is also a measure of complexity. However, it does not contain self-similar patterns as ApEn does. SampEn is the negative natural logarithm of the probability that if two sets of simultaneous data points of length *m* have distance *r*, then two sets of simultaneous data points of length *m+1* also have distance *r* for a given embedding dimension *m*, tolerance *r*, and number of data points *N*. SampEn is calculated for a given embedding dimension m, tolerance *r*, and number of data points *N*. And we demonstrate this by utilizing *SampEn (m, r, N)*. Assuming a time-series of length $N=\{x_1,x_2,x_3,....,x_N\}$ with constant interval of time τ. By defining the vector template of length *m*, such that $X_m(i)=\{x_i,x_{i+1},x_{i+2},....x_{i+m-1}\}$ and the Chebyshev distance $d[X_m(i),X_m(j)]$ $(i \ne j)$. Therefore, sample entropy can be defined as

$$SampEn=-\ln\left(\frac{P}{Q}\right) \tag{2}$$

where P = Number of vector template pairs having $d[X_{m+1}(i),X_{m+1}(j)]<r$, Q = Number of vector template pairs having $d[X_m(i),X_m(j)]<r$.

2.5.3 Permutation entropy

Permutation entropy is a measure of complexity used in the analysis of time series data. It is based on the concept of permutation of the order of values in a time series. In a time-series of length N, there are N! possible permutations. To calculate permutation entropy, first, the time series is transformed into a symbolic sequence by dividing the data into a set of ordinal patterns. Each ordinal pattern corresponds to the relative order of the values in a window of a certain length. Then, the frequency of occurrence of each ordinal pattern is calculated, and the Shannon entropy is calculated based on these frequencies. Permutation entropy has been found to be useful in detecting and characterizing complex dynamics in various systems, including physiological signals.

The permutation entropy [32, 33] (PeEn) of order $n \ge 2$ is expressed as $H(n)=-\sum p(\pi)\log p(\pi)$, where the sum is calculated for all *n!* permutations π of order *n*. This is the information obtained by comparing n consecutive time series data.

2.5.4 Multiscale entropy

Multiscale entropy (MultiEn) is a technique used to analyze time series data. It was developed as an extension of the sample entropy algorithm, which measures the amount of regularity or predictability in a signal. MSE takes into account the scale or resolution at which the signal is analyzed and is used to assess the complexity of a system across different temporal scales.

The MultiEn [34] algorithm involves dividing the time series into different temporal scales by applying a coarse-graining procedure. At each scale, the sample entropy is calculated and plotted against the scale factor. The resulting curve provides information about the complexity of the signal at different scales.

In a multiscale entropy (MultiEn) method, for a time-series, $\{x_1,....x_i,....,x_N\}$, initially, successive coarse-grained time series are generated by averaging an increasing number of data points in non-overlapping frames. Each coarse-gained time series element, y_j^τ, is calculated using the equation: $y_j^\tau=1\Big/\tau\sum_{i=(j-1)\tau+1}^{j\tau}x_i$, where τ denotes the scale factor and $1 \le j \le N/t$. The coarse-grained time series for scale *1* is just the original time series. Sample entropy (SampEn), a modification of the original ApEn statistics, was computed for each coarse-grained time series shown as a function of the scale factor τ.

2.5.5 Fuzzy entropy

Most of the time, fuzzy entropy [35] (FuzEn) may be used to assess the irregularity of a time series because it is accurate and independent of the size of the data. This method is somewhat slower as compared to sample entropy.

For a given FuzEn power *n* and tolerance *r*, the degree of similarity $d_{t_1t_2}$ can be calculated through a fuzzy function

$$\mu\left(d_{t_1t_2}, n, r\right) = \exp\left(-\left(d_{t_1t_2}\right)^n / r\right) \tag{3}$$

The function ϕ^m can be expressed as

$$\phi^m\left(x, n, r\right) = \frac{1}{N-m}\sum_{t_1=1}^{N-m}\frac{1}{N-m-1}\sum_{t_2=1, t_1\neq t_2}^{N-m}\exp\left(-\left(d_{t_1t_2}\right)^n / r\right) \tag{4}$$

The Fuzzy Entropy (FuzEn) can be mathematically expressed as a measure for a time series with an embedding dimension of m.

$$FuzEn(x, m, n, r) = -\ln\left(\frac{\phi^{m+1}}{\phi^m}\right) \tag{5}$$

2.5.6 Dispersion entropy

The dispersion entropy (DispEn) algorithm [36] has four basic steps for a given univariate signal of length $N : x = x_1, x_2, ..., x_N$. Applying the normal cumulative distribution function (NCDF) to express *x* to $y = y_1, y_2, ..., y_N$ from *0* to *1* is the initial step. Then, using a linear approach, we assign each y_j a positive integer between *1* and *c*. To accomplish this, we utilize $z_j^c = round(c.y_j + 0.5)$. For each component of the mapped signal, where z_j^c denotes j^{th} component of the time series (classified) and rounding entails either reducing or increasing a number to the next digit. For each embedding vector $z_i^{m,c}$ with embedding dimension m and time delay *d* is created according to $z_i^{m,c} = \{z_i^c, z_{i+d}^c, ..., z_{i+(m-1)d}^c\}$, where $i = 1, 2, ..., N-(m-1)d$. Each time series $z_i^{m,c}$ is expressed (mapped) to a dispersion pattern $\pi_{v_0v_1....v_{m-1}}$ where $z_i^c = v_0, z_{i+d}^c = v_1, ..., z_{i+(m-1)d}^c = v_{m-1}$. Number of different dispersion patterns that may be allocated to each time series $z_i^{m,c}$ is c^m, provided that the signal has m components and each component can be an integer between *1* and *c*. For every feasible dispersion pattern in c^m, the relative frequency is calculated as:

$$p\left(\pi_{v_0v_1....v_{m-1}}\right) = \frac{Number\left\{i \middle| i \le N-(m-1)d, z_i^{m,c} \text{ has type } \pi_{v_0v_1....v_{m-1}}\right\}}{N-(m-1)d} \tag{6}$$

The DE value with embedding dimension m, time delay *d*, and the number of classes *c* is calculated as follows, and always based on Shannon's concept of entropy:

$$DispEn(x, m, c, d) = -\sum_{\pi=1}^{c^m} p\left(\pi_{v_0v_1....v_{m-1}}\right).\ln\left(p\left(\pi_{v_0v_1....v_{m-1}}\right)\right) \tag{7}$$

2.5.7 Tsallis entropy

Tsallis entropy [37, 38] (TsEn)is expressed as $s_q(p_i) = \frac{j}{q-1}\left(1-\sum_i p_i^q\right)$, for a given discrete set of probabilities *pi*, with predefined condition $\sum_i p_i = 1$, and for any real number *q*. where *j* is a positive constant and *q* is a real parameter frequently referred to as the entropic-index. Putting limit as $q \to 1$, the recovered Boltzmann-Gibbs entropy is $S_{BG} = S_1(p) = -j\sum_i p_i \ln p_i$, *j* with the Boltzmann constant may be identified as j_B. For normally continuous probability distributions, Tsallis entropy can be defined as

$$S_q[p] = \frac{1}{q-1}\left(1 - \int (p(x))^q dx\right) \tag{8}$$

where *p(x)* is a probability density function.

2.5.8 Renyi entropy

Renyi entropy [37] (ReEn) of order β, where $\beta \geq 0$ and $\beta \neq 1$, is expressed as

$$H_\beta(Y) = \frac{1}{1-\beta}\log\left(\sum_{i=1}^{n} p_i^\beta\right) \tag{9}$$

Here, Y is a random variable discrete in nature with probable outcomes in the set $B = \{y_1, y_2, ..., y_N\}$ and corresponding probabilities $p_i = \Pr(Y = y_i)$ for $i = 1, 2, ..., n.$

2.5.9 Shannon entropy

Shannon's Entropy [39] (ShEn) is just a variable's "amount of information." In information theory, the entropy of a random variable represents the average level of "information," "surprise," or "uncertainty" inherent to the variable's potential outcomes. Given a discrete random variable X, whose values are the letters of the alphabet $\mathcal{X}$, and whose distribution follows $p: \mathcal{X} \to [0,1]$:

$$H(x) := -\sum_{x \in \chi} p(x) \log p(x) = \mathbb{E}\left[-\log p(X)\right] \tag{10}$$

where Σ is the total range of potential values for the variable. For various purposes, the logarithm's base might be chosen in a different way. Bits (or "shannons") are represented by base *2*; "natural units" (nat) are represented by base *e*; and "dits," "bans," or "hartleys" are represented by base *10*. The expected value of a variable's self-information can serve as an alternative definition of entropy.

2.5.10 Lempel–Ziv complexity

The Lempel–Ziv complexity [40] (LZC) is related to the Kolmogorov complexity, however it employs simply the recursive copy function. The principle underpinning this complexity metric serves as the basis for many lossless data compression algorithms. Even though it is based on the simple word copying principle, this complexity measure is not overly restrictive in that it satisfies the key characteristics expected of a measure of this kind: sequences with a certain regularity do not have an excessive complexity, and complexity increases as the sequence increases in length and irregularity. Binary sequences and text, such as song lyrics or writing, can both have their repetitiveness measured using the Lempel-Ziv complexity. It has also been demonstrated that real-world data estimations of fractal dimension correspond with Lempel-Ziv complexity.

2.5.11 Detrended fluctuation analysis

Detrended fluctuation analysis [41] (DFA) is a technique used in stochastic processes, chaos theory, and time series analysis to determine the statistical self-affinity of a signal. It is helpful for analyzing time series that seem to be *1/f* noise or long-memory operations. The resultant exponent is comparable to the Hurst exponent, with the exception that DFA can also be applied to non-stationary signals whose underlying statistics include mean and variance or dynamics. It is connected to spectrum techniques like autocorrelation and Fourier transform. Considering a time series y_t of length *N*, where $t \in \mathbb{N}$, and let the mean value of the series is denoted as $\langle y \rangle$. This is transformed into an unbounded process *Yt* through integration or summation i.e.,

$$Y_t = \sum_{i=1}^{t} \left(y_i - \langle y \rangle\right) \tag{11}$$

Y_t is called cumulative sum. Y_t is split into time windows with n samples each, and a local least squares straight-line fit (the local trend) is found by finding the point where the squared errors in each time window are the smallest. Let X_t be the piecewise sequence of straight-line fits that is made as a result. Then, the fluctuation, which is the root-mean-square deviation from the trend, is found:

$$F(n) = \sqrt{\frac{1}{N}\sum_{t=1}^{N}\left(Y_t - X_t\right)^2} \tag{12}$$

2.5.12 Hurst exponent

Time series' long-term memory is evaluated using the Hurst exponent [42] (HuEx). It is concerned with time series autocorrelations and the rate at which they decrease as the lag between pairs of values increases. The Hurst exponent was first used in hydrology to determine the best dam size for the Nile River's volatile rain and drought conditions, which had been observed over a long period of time. The term "Hurst exponent" or "Hurst coefficient" refers to the lead researcher in these studies, Harold Edwin Hurst (1880-1978); the use of the standard notation H for the coefficient also refers to him. According to the asymptotic behaviour of the rescaled range as a function of a time series' duration, the Hurst exponent, or H, is defined as,

$$\mathbb{E}\left[\frac{R(n)}{S(n)}\right] = Cn^{H} \text{ as } n \to \infty \tag{13}$$

where; *R(n)* is the span of first n aggregate deviations from the mean, *S(n)* is the sum of the first n number of standard deviations, $\mathbb{E}[x]$ is the expected value, *n* is the total number of data points of that time series, *C* is a constant.

2.5.13 Correlation dimension

The correlation dimension [43] (CD), which is frequently referred to as a particular kind of fractal dimension, is a measure of the dimensionality of the space occupied by a collection of random points in chaos theory. The correlation dimension's true utility is in determining the dimensions of fractal objects. In an m-dimensional space, any set of N points $\vec{y}(i) = \left[y_1(i), y_2(i), ..., x_m(i)\right], i = 1, 2, ..., N$, then the correlation integral *C(ε)* is estimated by: $C(\varepsilon) = \lim_{N\to\infty} \frac{g}{N^2}$. where g represents the total amount of point pairings where the distance between them is smaller than distance ε. As the number of points approaches infinity and their separation approaches zero, the correlation integral for small values of will take the form: $C(\varepsilon) \sim \varepsilon^{v}$. A log-log graph of the correlation integral versus ε will produce an estimate of v if the points are numerous and uniformly spaced. This concept can be comprehended qualitatively by recognizing that for higher-dimensional objects, there will be more ways for points to be close to one another, and so the number of pairs that are close together will increase more quickly for higher dimensions.

2.5.14 Higuchi fractal dimension

A rough estimate of the box-counting dimension of the graph of a real-valued function or time series is the Higuchi fractal dimension [44] (HFD). This figure was calculated using an algorithmic approximation; hence the Higuchi approach is also mentioned. For a time-series $Y : \{1, 2, ..., N\} \to \mathbb{R}$ containing of *N* observations and a parameter $k_{\max} \geq 2$ the HFD of *Y* can be expressed as: for every $k \in \{1, 2, ..., k_{\max}\}$ and $j \in \{1, 2, ..., k\}$ defining the length

$$L_j(k) = \frac{N-1}{\left\lfloor \frac{N-j}{k} \right\rfloor k^2} \sum_{i=1}^{\left\lfloor \frac{N-j}{k} \right\rfloor} \left| Y_N\left(j+ik\right) - Y_N\left(j+(i-1)k\right) \right| \tag{14}$$

L(k) is determined by the mean of the *k* lengths $L_1(k), ..., L_k(k)$,

$$L(k) = \frac{1}{k}\sum_{j=1}^{k} L_j(k) \tag{15}$$

The slope of the linear function that best fits the data points $\left\{\left(\log\frac{1}{k}, \log L(k)\right)\right\}$ is known to be Higuchi fractal dimension of the time-series *Y*.

2.5.15 Lyapunov exponent

Lyapunov exponent is a measure of the rate of divergence or convergence of nearby trajectories in a nonlinear dynamical system. In a nonlinear system, small perturbations in the initial conditions can lead to significantly different trajectories over time. The Lyapunov exponent measures the average rate at which these perturbations grow or decay exponentially along the trajectory. A positive Lyapunov exponent indicates that the nearby trajectories diverge exponentially, whereas a negative Lyapunov exponent indicates that they converge exponentially towards a common attractor. The rate at which two infinitesimally close trajectories separate is represented mathematically by the Lyapunov exponent, also known as the Lyapunov characteristic exponent [45] (LE) of a dynamical system. Two phase-space trajectories with initial separation vectors δZ_0 diverge quantitatively at a rate defined by $\left|\delta Z(t)\right| \approx e^{\lambda t}\left|\delta Z_0\right|$ where

λ is Lyapunov exponent. For various initial separation vector orientations, the rate of separation can vary. Thus, a spectrum of Lyapunov exponents exists, the number of which is proportional to the dimension of the phase space.

2.6 Statistical analysis

Using conventional procedures such as the Shapiro-Wilk test or the Kolmogorov-Smirnov test, the normal distribution of the data may be examined. In this experimental process the Shapiro-Wilk test was performed in both the study I and II to assess whether the distribution of data was normal or not. As usually most of the entropies and the complexity parameters were not distributed normally, therefore different suitable non-parametric tests were emphasized to measure the systematic differences among both the sessions in study I and among the three different sessions of the day in study II for EOG data acquired by the horizontal channel of Biopac MP 45 system. Beside the parametric test, non-parametric Wilcoxon test and Friedman test were also performed to assess the systematic differences among sessions in study I and as well as in study II. The Post hoc analysis was done by plug in the Tukey-Kramer test to compare and investigate the difference of complexity parameters in different sessions of the day. In order to execute the Tukey-Kramer test, morning-afternoon (MR-AN), morning-evening (MR-EV) and afternoon-evening (AN-EV) paired data i.e., entropies and complexity parameters were compared. To determine the agreement between the normal state and stressed state in terms of the different complexity parameters the Bland-Altman plots [46, 47] with 95% LOA were used. LOA values imply that 95% of the data points fall within the bounds of the mean difference and are used to visually examine the level of agreement between two states of fatigue. A two-way mixed intraclass correlation coefficient (ICC) was utilized to examine the relatedness or reliability index. It was used to assess the reliability of individual complexity parameter for both the sessions of fatigue in study-I and as well as for three different sessions of day in study-II. The reliability is classified as poor when ICC is less than 0.5, moderate when it is in-between 0.5-0.75, good when it is in-between 0.75-0.9 and excellent when it is above 0.9. Correlation analyses determine the degree of association between two variables. Non-parametric Kendall's Tau and Spearman's rank correlation coefficient were examined to evaluate statistical relationships between all the complexity parameters with ApEn, TsEn, ShEn, LZC. All the statistical tests were examined at a threshold of 5% significance level and were performed using MATLAB Release 2018a.

3. Results and Discussion

In this experimental process two studies were performed. In study-I, a well-designed inferetial statistical analysis of EOGs for both the sessions in connection with fatigue and drowsiness was performed for time domain entropy, frequency domain entropy and other complexity parameters of different patterns of the cue movements i.e., RCW, RAC, TCW and TAC separately. Those analyses are depicted clearly in Table 3, Table 4, Table 5 and Table 6 respectively. All the entropies and complexity parameters are expressed in mean ± SEM along with their confidence interval range of 95%. A parametric t-test and a non-parametric Wilcoxon test were conducted, but as the most of complexity parameters were not distributed normally, the non-parametric Wilcoxon test was favored for determining the difference between two sessions. Conclusions are drawn at 5% ($p \leqslant 0.05$) significance level, while $p>0.05$ are considered as non-significant (NS).

The effect of intensive cognitive activity on different complexity parameters for different pattern of cue movements on morning and evening EOGs are clearly reflected in the said tabular descriptions. In Table 3, for RCW, almost all the complexity parameters except SampEn and HuEx exhibit clear difference between entropies and complexity parameters between morning and evening sessions with significance level of 5%.

Table 3. The comparison of complexity parameters of EOGs with cue pattern RCW between normal state and stressed state mentioned in study-I.

Complexity parameters	Morning		Evening		Wilcoxon test (p-value)	t test (p-value)	ICC
	Mean ± SEM	95%CI	Mean ± SEM	95%CI			
Time domain entropy							
ApEn	2.32±0.15	2.01-2.64	2.95±0.17	2.60-3.30	<0.0001	<0.0001	0.89
SampEn	2.25±0.14	1.96-2.55	2.46±0.17	2.11-2.82	0.8793 **(NS)**	0.0654 **(NS)**	0.87
PeEn	4.34±0.22	3.91-4.77	5.38±0.21	4.96-5.80	<0.0001	<0.0001	0.87
MultiEn	2.85±0.19	2.46-3.23	5.25±0.23	4.79-5.71	<0.0001	<0.0001	0.79
FuzEn	4.91±0.21	4.48-5.34	3.80±0.22	3.35-4.25	<0.0001	<0.0001	0.85
DispEn	6.15±0.10	5.95-6.35	5.62±0.13	5.35-5.89	<0.0001	<0.0001	0.73
Frequency domain entropy							
TsEn	6.66±0.22	6.20-7.11	8.29±0.16	7.97-8.61	<0.0001	<0.0001	0.84
ReEn	3.37±0.21	2.94-3.79	4.51±0.20	4.10-4.91	<0.0001	<0.0001	0.89
ShEn	3.53±0.22	3.09-3.98	2.03±0.17	1.68-2.39	<0.0001	<0.0001	0.89
Others							
LZC	2.10±0.15	1.79-2.41	3.38±0.19	2.99-3.77	<0.0001	<0.0001	0.83
DFA	5.42±0.16	5.10-5.74	4.93±0.17	4.60-5.26	<0.0001	<0.0001	0.86
HuEx	3.75±0.18	3.40-4.11	3.93±0.19	3.56-4.30	0.3391 **(NS)**	0.2681 **(NS)**	0.76
CD	4.68±0.20	4.28-5.08	5.17±0.18	4.80-5.54	0.0301	0.0158	0.64
HFD	2.38±0.16	2.06-2.70	3.47±0.22	3.03-3.90	<0.0001	<0.0001	0.83
LE	2.77±0.16	2.43-3.10	4.42±0.20	4.01-4.84	<0.0001	<0.0001	0.89

Table 4. The comparison of complexity parameters of EOGs with cue pattern RAC between normal state and stressed state mentioned in study-I.

Complexity parameters	Morning		Evening		Wilcoxon test (p-value)	t test (p-value)	ICC
	Mean ± SEM	95%CI	Mean ± SEM	95%CI			
Time domain entropy							
ApEn	2.33±1.86	1.99-2.66	2.55±1.87	2.21-2.89	0.4763 **(NS)**	0.0950 **(NS)**	0.82
SampEn	3.04±1.46	2.78-3.30	2.26±1.79	1.93-2.58	<0.0001	<0.0001	0.77
PeEn	4.67±2.35	4.25-5.10	5.42±2.43	4.99-5.86	<0.0001	<0.0001	0.83
MultiEn	3.17±2.12	2.79-3.56	5.78±3.15	5.21-6.35	<0.0001	<0.0001	0.79
FuzEn	3.75±2.12	3.37-4.14	3.43±2.42	2.99-3.87	0.0237	0.0301	0.86
DispEn	5.76±1.20	5.54-5.97	4.83±1.54	4.55-5.11	<0.0001	<0.0001	0.65
Frequency domain entropy							
TsEn	7.64±2.07	7.26-8.01	7.98±1.88	7.64-8.32	0.0892 **(NS)**	0.0275	0.77
ReEn	3.62±2.13	3.23-4.01	4.29±2.25	3.89-4.70	<0.001	<0.0001	0.84
ShEn	3.14±2.35	2.71-3.56	2.31±2.09	1.93-2.69	<0.0001	<0.0001	0.82
Others							
LZC	1.44±1.39	1.18-1.69	3.16±2.25	2.75-3.57	<0.0001	<0.0001	0.76
DFA	5.43±1.88	5.09-5.77	6.04±1.86	5.71-6.38	<0.0001	<0.0001	0.85
HuEx	3.48±1.91	3.13-3.82	4.83±2.49	4.38-5.28	<0.0001	<0.0001	0.68
CD	4.17±1.80	3.84-4.49	6.17±2.16	5.78-6.56	<0.0001	<0.0001	0.69
HFD	2.34±1.93	1.99-2.68	3.60±2.27	3.19-4.01	<0.0001	<0.0001	0.76
LE	2.72±2.09	2.34-3.10	3.60±2.42	3.16-4.03	<0.0001	<0.0001	0.90

For RAC, Table 4 justifies the significant difference between entropies and complexity parameters between morning and evening sessions with $p<0.05$ except ApEn, and TsEn.

Table 5. The comparison of complexity parameters of EOGs with cue pattern TCW between normal state and stressed state mentioned in study-I.

Complexity parameters	Morning		Evening		Wilcoxon test (p-value)	t test (p-value)	ICC
	Mean ± SEM	95%CI	Mean ± SEM	95%CI			
Time domain entropy							
ApEn	2.67±0.16	2.35-3.00	3.24±0.17	2.90-3.58	<0.001	<0.001	0.74
SampEn	2.68±0.17	2.34-3.02	2.54±0.19	2.17-2.92	0.0464	0.4408 **(NS)**	0.69
PeEn	4.81±0.19	4.43-5.18	5.16±0.21	4.73-5.58	0.0278	0.0256	0.83
MultiEn	4.49±0.26	3.98-5.00	4.50±0.20	4.09-4.90	0.7100 **(NS)**	0.9709**(NS)**	0.80
FuzEn	3.92±0.18	3.57-4.27	3.16±0.20	2.76-3.57	<0.0001	<0.0001	0.83
DispEn	6.40±0.15	6.11-6.70	5.01±0.14	4.74-5.28	<0.0001	<0.0001	0.38
Frequency domain entropy							
TsEn	8.05±0.14	7.78-8.33	8.26±0.17	7.92-8.59	0.0079	0.0732 **(NS)**	0.85
ReEn	4.13±0.18	3.77-4.49	4.64±0.20	4.24-5.05	<0.001	<0.0001	0.87
ShEn	2.35±0.16	2.03-2.67	1.91±0.17	1.57-2.25	<0.0001	<0.001	0.86
Others							
LZC	2.37±0.15	2.08-2.66	3.49±0.20	3.09-3.89	<0.0001	<0.0001	0.71
DFA	5.39±0.19	5.02-5.76	3.53±0.15	3.24-3.82	<0.0001	<0.0001	0.68
HuEx	5.00±0.17	4.66-5.35	4.54±0.17	4.20-4.88	0.0028	0.0113	0.64
CD	5.33±0.19	4.95-5.70	5.42±0.18	5.06-5.78	0.8875 **(NS)**	0.6023 **(NS)**	0.72
HFD	3.84±0.20	3.44-4.24	3.82±0.19	3.43-4.20	0.1620 **(NS)**	0.8847 **(NS)**	0.79
LE	3.11±0.16	2.81-3.42	4.26±0.20	3.85-4.66	<0.0001	<0.0001	0.87

Table 6. The comparison of complexity parameters of EOGs with cue pattern TAC between normal state and stressed state mentioned in study-I.

Complexity parameters	Morning		Evening		Wilcoxon test (p-value)	t test (p-value)	ICC
	Mean ± SEM	95%CI	Mean ± SEM	95%CI			
Time domain entropy							
ApEn	3.43±0.16	3.10-3.75	3.30±0.16	2.98-3.62	0.0055	0.4474 **(NS)**	0.63
SampEn	2.92±0.14	2.64-3.19	2.98±0.18	2.62-3.34	0.3498 **(NS)**	0.7440 **(NS)**	0.50
PeEn	4.55±0.20	4.15-4.95	4.86±0.19	4.48-5.23	0.0633 **(NS)**	0.0327	0.84
MultiEn	3.96±0.23	3.50-4.42	5.76±0.27	5.23-6.29	<0.0001	<0.0001	0.82
FuzEn	4.65±0.22	4.21-5.09	3.40±0.21	3.00-3.81	<0.0001	<0.0001	0.88
DispEn	4.91±0.11	4.67-5.13	5.24±0.15	4.94-5.53	0.0069	0.0214	0.59
Frequency domain entropy							
TsEn	7.33±0.18	6.97-7.69	8.12±0.17	7.77-8.47	<0.0001	<0.0001	0.85
ReEn	4.48±0.22	4.40-4.92	4.91±0.21	4.49-5.32	0.0243	0.0066	0.85
ShEn	3.04±0.20	2.63-3.44	2.07±0.18	1.72-2.42	<0.0001	<0.0001	0.88
Others							
LZC	3.15±0.19	2.77-3.53	4.15±0.16	3.82-4.48	<0.0001	<0.0001	0.54
DFA	4.03±0.19	3.64-4.43	4.83±0.15	4.51-5.15	<0.0001	<0.001	0.56
HuEx	4.65±0.18	4.28-5.01	4.97±0.20	4.55-5.38	0.2273 **(NS)**	0.0924 **(NS)**	0.70
CD	5.65±0.14	5.36-5.93	6.51±0.18	6.14-6.88	<0.0001	<0.0001	0.63
HFD	3.47±0.19	3.09-3.84	3.48±0.18	3.10-3.85	0.1149 **(NS)**	0.9636 **(NS)**	0.66
LE	2.77±0.16	2.45-3.10	3.80±0.20	3.41-4.20	<0.0001	<0.0001	0.85

For TCW, from Table 5, the complexity parameters like ApEn, PeEn, FuzEn, DispEn, ReEn, ShEn, LZC, DFA, HuEx and LE are showing prominent differences between the two sessions with threshold level $p<0.05$. Whereas the other complexity parameters like MultiEn, CD and HFD are showing non-significant differences for $p<0.05$. SampEn and TsEn of EOGs are significant for non-parametric Wilcoxon test (for $p<0.05$) but showing non-significant for parametric t test.

For TAC, in Table 6, the MultiEn, FuzEn, DispEn, TsEn, ReEn, ShEn, LZC, DFA, CD, LE are showing significant differences at 5% significance level. The rests time domain entropies and others complexity parameters are non-significant. ApEn, is significant for non-parametric Wilcoxon test but non-significant for t test. The PeEn is non-significant for non-parametric Wilcoxon test but significant for parametric t test.

Fig. 5 shows the violin plots for all the time domain, frequency domain and others complexity parameters of EOGs for both the morning and evening sessions under RCW cue movement. Fig. 6 shows the reference violin plot. Generally numeric data can be plotted using violin plots, which are a combination of the box plot and the kernel density plot. Visualizing the distribution of the data and the probability density of it may be done with the use of a violin plot. The p values given in Table 3 can be understood by analyzing violin plots shown in Fig. 5. Both the violins under the plots of SampEn and HuEx for morning and evening sessions are almost overlapping with each other and suggests no significant difference between them. The term "overlapping" refers to the phenomenon of either median overlapping or box overlapping. When the medians of two boxplots overlap or are in close proximity, it suggests that the central tendencies of the distributions are comparable. When the boxes of two boxplots overlap, it implies that there is an overlap in the middle 50% of the data, which suggests similarity. Figures 5 and 7-9 depict a total of 15 pairs of violins for each of the four cue movements, namely RCW, RAC, TCW, and TAC respectively. For others complexity parameters as the boxes are not completely overlapping with each other, it signifies that there are prominent differences in EOGs between the morning and evening sessions. The other violin plots are also depicted for RAC, TCW and TAC in Fig. 7-9 respectively.

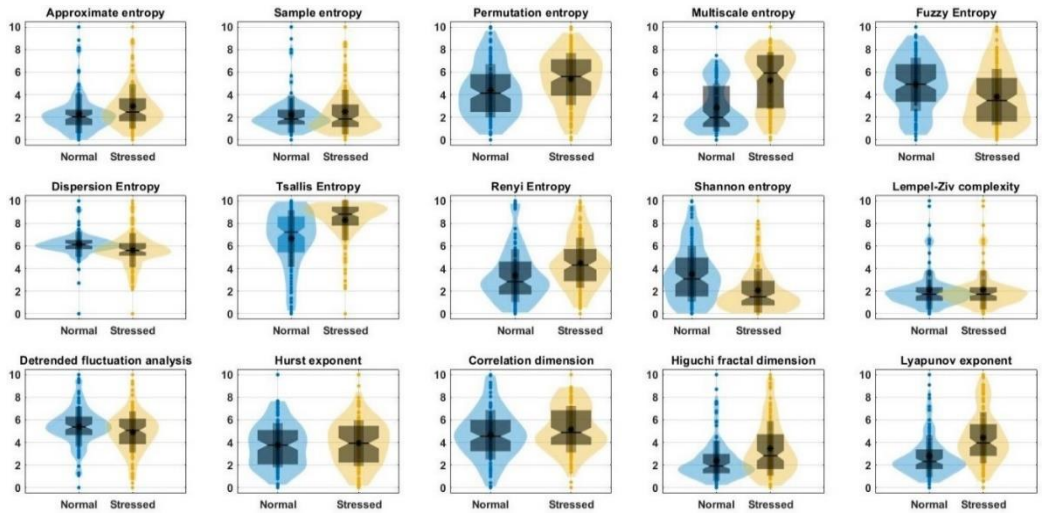

Fig. 5. Violin plots for time domain, frequency domain and the others complexity parameters of RCW EOGs under normal and stressed states.

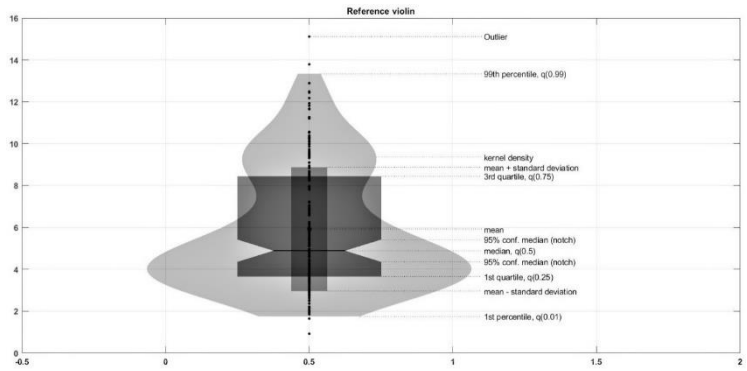

Fig.6. Reference violin plot.

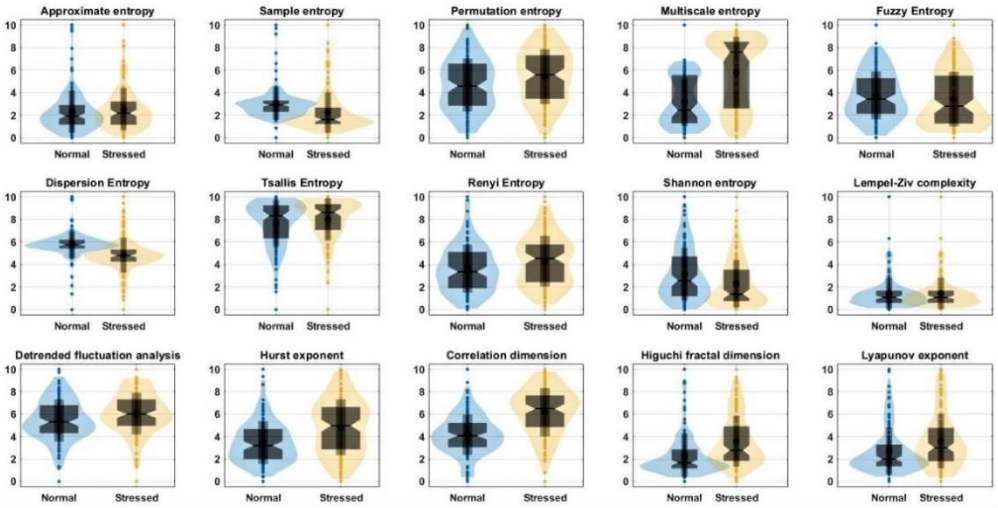

Fig. 7. Violin plots for time domain, frequency domain and the others complexity parameters of RAC EOGs under normal and stressed states.

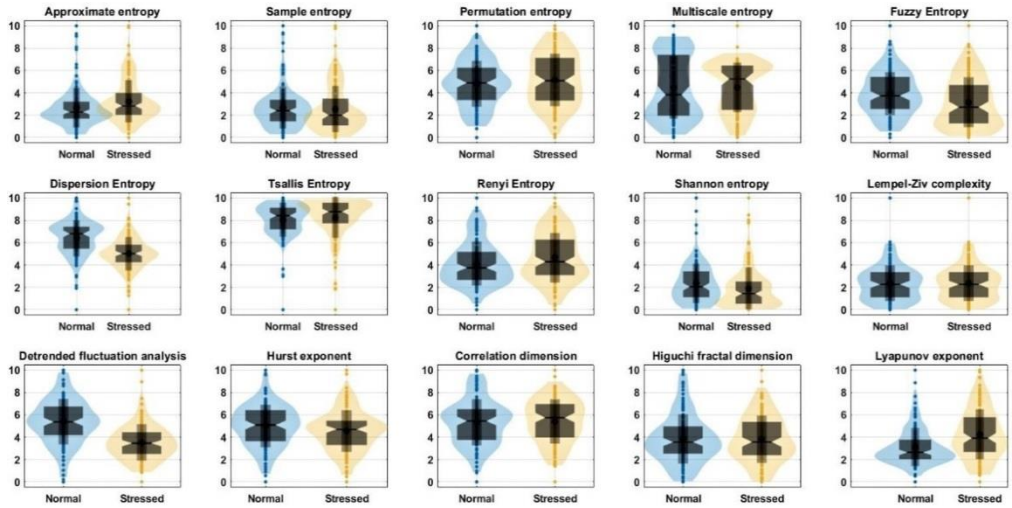

Fig. 8. Violin plots for time domain, frequency domain and the others complexity parameters of TCW EOGs under normal and stressed

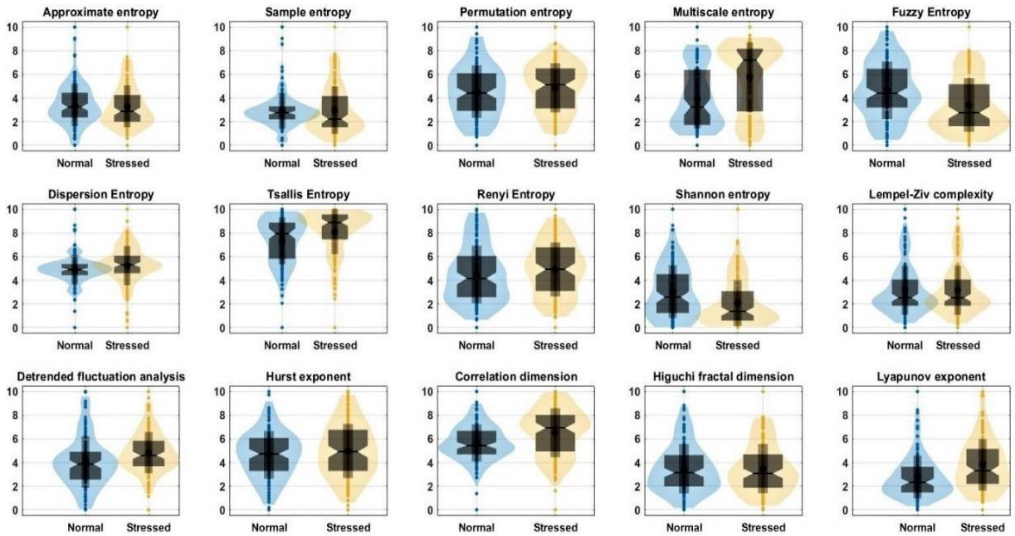

Fig. 9. Violin plots for time domain, frequency domain and the others complexity parameters of TAC EOGs under normal and stressed states.

Upon examination of Figure 7 and Table 4, it can be discerned that in the case of RAC cue movement, the violins of the morning and evening sessions exhibit overlapping measurements of ApEn and TsEn. However, the remaining violins do not overlap completely, suggesting stress level variations between the morning and evening sessions. Consequently, the Wilcoxon test yielded a non-significant outcome for the aforementioned pair of complexity

parameters. The results obtained from Fig. 8 and Table 5 regarding the movement of TCW cues indicate that MultiEn, CD, and HFD exhibit similarities between morning and evening sessions, with no significant differences observed. Upon examination of Fig. 9 and Table 6 pertaining to TAC cue movement, it can be observed that both SampEn and PeEn exhibit overlapping characteristics, suggesting the absence of significant differences in stress levels between morning and evening sessions.

ICCs were measured to detect the reliability of an experimental process. ICC ranged from 0.73 to 0.89, from 0.65 to 0.90, from 0.38 to 0.87 and from 0.50 to 0.88 for RCW, RAC, TCW and TAC respectively. This means that random and systematic errors were reported [48] and also varies from 11%-36%, 10%-35%, 13%-62% and 12%-50% for RCW, RAC, TCW and TAC respectively. The highest reliability was reported as 0.89 for ApEn, ReEn, ShEn, LE, 0.90 for LE, 0.87 for ReEn, LE and 0.88 for FuzEn, ShEn in RCW, RAC, TCW and TAC respectively.

For estimating the agreement between the time domain, frequency domain and others complexity parameters of EOGs under morning and evening sessions, the Bland-Altman plot is used. It can be used to identify any systematic bias or variability between the entropies and complexity parameters of EOGs at morning and evening sessions, as well as any outliers or extreme differences. The Bland-Altman plots for time domain, frequency domain and others complexity parameters for RCW, RAC, TCW and TAC are depicted in Fig. 10-13 respectively.

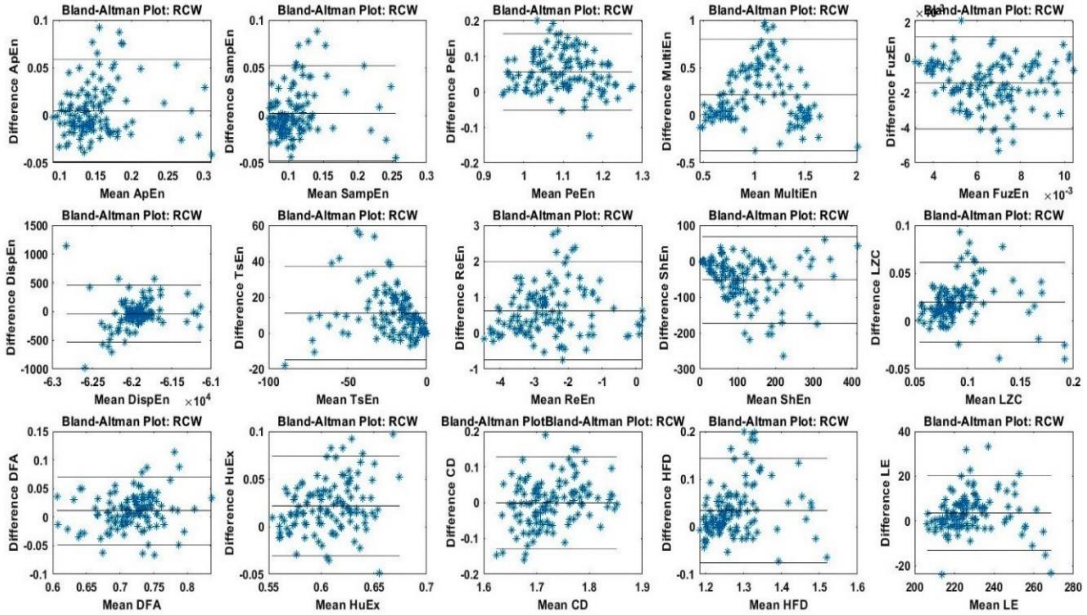

Fig. 10. Bland-Altman plots for time domain, frequency domain and the others complexity parameters of RCW EOGs.

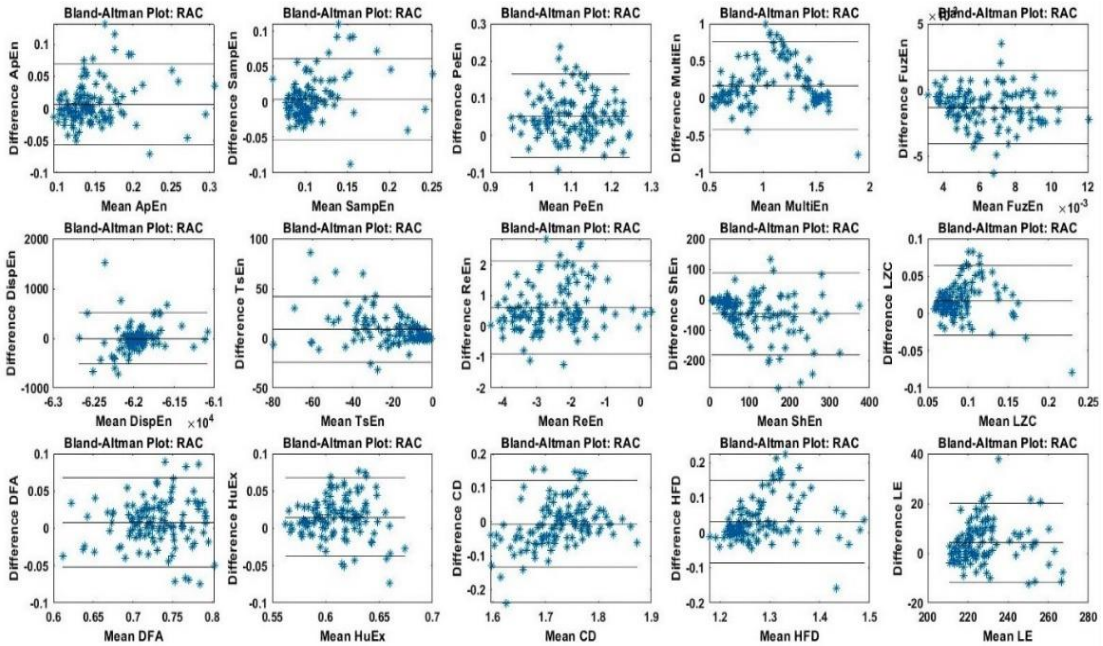

Fig. 11. Bland-Altman plots for time domain, frequency domain and the others complexity parameters of RAC EOGs.

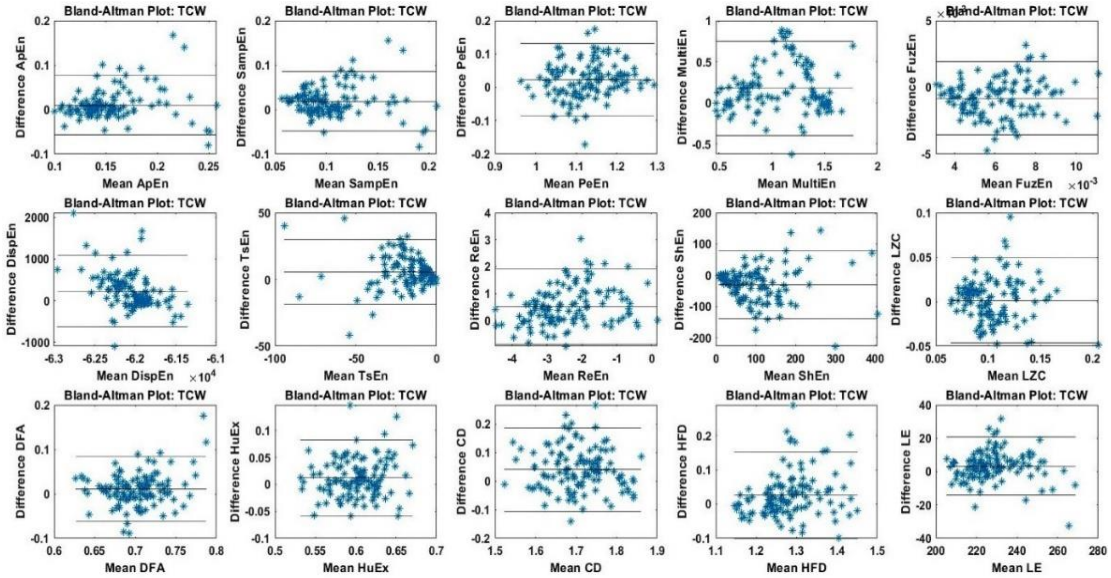

Fig. 12. Bland-Altman plots for time domain, frequency domain and the others complexity parameters of TCW EOGs

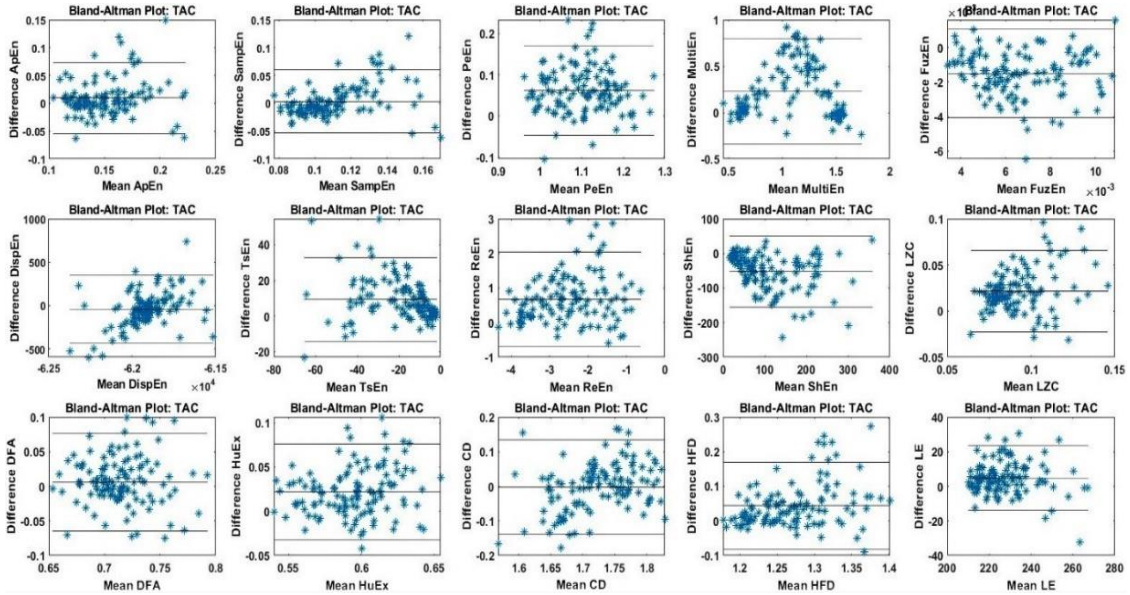

Fig. 13. Bland-Altman plots for time domain, frequency domain and the others complexity parameters of TAC EOGs

Bland-Altman plot is basically a scatter plot and can be used to compare entropies and complexity parameters among morning and evening sessions to comment on fatigue and drowsiness of the participants. To comprehend variable dispersion, a scatterplot is created using the X-axis (mean) and Y-axis (difference). In this plot, mean difference or mean bias is drawn at middle of Y-axis. The outer lines (i.e., the upper limit and lower limit) as 95% of LOA (limits of agreement) are calculated by mean ± 1.96 x standard deviation of the differences. If the data points are very close to zero line, then it indicates that there is a good level of agreement between the entropies and complexity parameters among the morning and evening sessions under consideration, otherwise it is treated as weak agreement. Strong agreement shows that there is no proportional bias on the distribution of data around the mean difference line. After getting the plots, it can be interpreted by linear regression method. The difference in entropies and complexity parameters expressed a nearly symmetrical distribution around the zero-line, indicating the absence of systematic changes as a function of the mean for DispEn, DFA in RCW; mean for SampEn, DispEn, TsEn in RAC; mean for ApEn, SampEn, TsEn, DFA in TCW and mean for ApEn, DispEn, in TAC. Other entropies and fatigue complexity indices like ApEn, SampEn, PeEn, MultiEn, FuzEn, TsEn, ReEn, ShEn, LZC, HuEx,, CD, HFD, LE in RCW; ApEn, PeEn, MultiEn, FuzEn, ReEn, ShEn, LZC, DFA, HuEx,, CD, HFD, LE in RAC; PeEn, MultiEn, FuzEn, DispEn, ReEn, ShEn, LZC, HuEx,, CD, HFD, LE in TCW and SampEn, PeEn, MultiEn, FuzEn, TsEn, ReEn, ShEn, LZC, DFA, HuEx,, CD, HFD, LE in TAC indicate a systematic change, i.e., heteroscedasticity for the morning and evening session entropies and fatigue complexity indices expressing differences in stress conditions obtained from morning and evening sessions. Hence, it may be concluded that the Bland-Altman plots accurately reflect the differences between fatigue complexity indices obtained from EOGs of morning and evening sessions. As depicted in Table 7, regression analysis is used to

further investigate weak agreements among entropies and complexity parameters. It is observed for SampEn, TsEn, ShEn, DFA, HuEx, CD & HFD in RCW cue movement, for ApEn, SampEn, TsEn, ShEn, CD & HFD in RAC cue movement, for DispEn, ReEn, DFA & HFD in TCW cue movement, and SampEn, DispEn, TsEn, ReEn, ShEn, LZC, HuEx, CD & HFD in TAC cue movement are showing weak agreements between the EOGs of morning and evening sessions.

Table 7. Comparative statistics (p-values) of linear regression among RCW, RAC, TCW, TAC cue movements for post Bland-Altman normal and stressed states under study-I.

Complexity parameters	**RCW (p-value)**	**RAC (p-value)**	**TCW (p-value)**	**TAC (p-value)**	**Weak agreements or statistically significant differences**
Time domain entropy					
ApEn	0.1340 **(NS)**	0.0359	0.0963 **(NS)**	0.1790 **(NS)**	**RAC**
SampEn	0.0485	0.0013	0.9980 **(NS)**	<0.0001	**RCW, RAC, TAC**
PeEn	0.2330 (NS)	0.7830 **(NS)**	0.1360 **(NS)**	0.7520 **(NS)**	NONE
MultiEn	0.9000 (NS)	0.8090 **(NS)**	0.5560 **(NS)**	0.7330 **(NS)**	NONE
FuzEn	0.3160 (NS)	0.1990 **(NS)**	0.2370 **(NS)**	0.4730 **(NS)**	NONE
DispEn	0.0970 (NS)	0.0553 **(NS)**	<0.0001	<0.0001	**TCW, TAC**
Frequency domain entropy					
TsEn	0.0230	<0.0001	0.4540 **(NS)**	0.0054	**RCW, RAC, TAC**
ReEn	0.2760 **(NS)**	0.0690 **(NS)**	0.0028	0.0151	**TCW, TAC**
ShEn	0.0243	0.0005	0.6670 **(NS)**	0.0013	**RCW, RAC, TAC**
Others					
LZC	0.634 **(NS)**	0.7720 **(NS)**	0.7040 **(NS)**	0.0021	**TAC**
DFA	0.0382	0.0680 **(NS)**	0.0098	0.3250 **(NS)**	**RCW, TCW**
HuEx	0.0017	0.9580 **(NS)**	0.2130 **(NS)**	0.0396	**RCW, TAC**
CD	0.0012	<0.0001	0.3640 **(NS)**	<0.0001	**RCW, RAC, TAC**
HFD	0.0081	0.0086	0.0116	0.0003	**RCW, RAC, TCW, TAC**
LE	0.8280 (NS)	0.6130 **(NS)**	0.7730 **(NS)**	0.3700 **(NS)**	NONE

In study-II, the same inferential statistical analysis for time domain, frequency domain and other complexity parameters of EOGs of morning, afternoon and evening was performed to investigate fatigue and drowsiness. The said analysis is shown in Table 8. All the entropies and complexity parameters are expressed in mean ± SEM along with their confidence interval range of 95% as done in study-I. A non-parametric Friedman test and a parametric ANOVA test were conducted, but as the most of complexity parameters were not distributed normally, the non-parametric Friedman test was normally favoured for determining the difference between entropies and complexity parameters under morning, afternoon and evening sessions. Similarly, conclusions are drawn at 5% ($p \leq 0.05$) significance level, while $p > 0.05$ are taken as non-significant (NS).

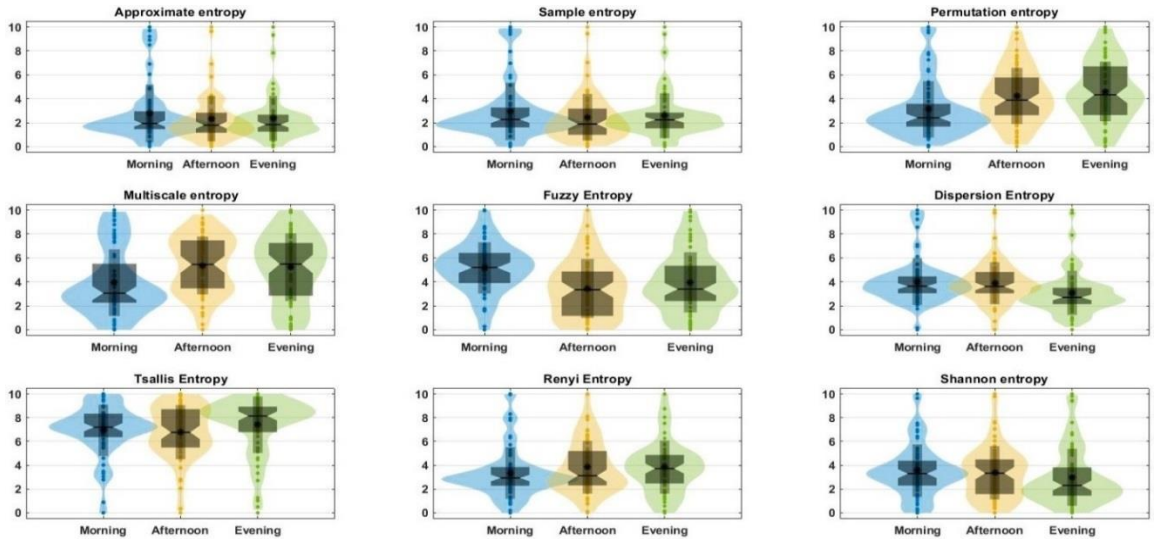

Fig. 14. Violin plots for time domain and frequency domain entropies of EOGs recorded in morning (MR), afternoon (AN) and evening.

The outcome of intensive cognitive activity on the participants is reflected on the different complexity parameters in different sessions of the day. From the Table 8 it is evident that change in SampEn (p=0.0901) non-significant. Except SampEn, all the time domain, frequency domain entropies and the others complexity parameters are showing significant differences in recorded EOGs on different sessions of the day. The Tukey-Kramer test approves statistical variations between all the possible groups i.e., MR-AN, MR-EV and AN-EV having $p<0.05$. ApEn has $p=0.0439$, with

significant difference in MR-AN (p=0.0363), MultiEn has values p<0.001, with significant differences both in MR-AN (p=0.0066) and MR-EV (p=0.0017). DispEn is possessing p<0.0001, with clear differences both in MR-EV (p<0.0001) and AN-EV (p<0.0001). There are significant differences for all the frequency domain entropies at p<0.05 and differences are showing significant in MR-EV and also in AN-EV (except ReEn). In the others complexity parameters like LZC has p<0.0001 with clear differences in MR-AN (p< 0.0001) and AN-EV (p<0.0001), HuEx has p=0.0042 with clear difference in MR-AN (p=0.0030), CD has p<0.0001 with strong difference in MR-AN (p<0.0001), HFD is possessing p<0.0001 with clear differences in MR-EV (p<0.0001) and AN-EV (p<0.0001) and LE has p<0.0001 with strong differences in MR-AN (p<0.0001) and MR-EV (p<0.0001).

Fig. 14 shows the violin plots for all the time domain and frequency domain entropies of recorded EOGs at three different sessions i.e., morning (MR), afternoon (AN) and evening (EV). The p values depicted in Table 8 is likely to be interpreted by analyzing violin plots shown in Fig. 14. All the violins under the plots under SampEn for three different sessions are almost overlapping with each other and confirms no significant differences between them. For the case of the other entropies under time and frequency domains, there are distinct differences in their medians of the box-violin plots, concludes that there are significant changes in stress levels of participants among the different sessions of the day which suggest the onset of drowsiness and fatigue in their muscles.

Fig. 15 shows the violin plots for all the others complexity parameters of recorded EOGs at three different sessions i.e., morning (MR), afternoon (AN) and evening (EV). The depicted p (probability) values in Table 8 can probably be understood by observing the violin plots in Fig. 15. In the complexity parameters for each session of the day, a box-violin plot is used to illustrate how the magnitudes are generally distributed over their quartiles. Most of the violins under the plots of the other complexity parameters show clear differences in their medians. This settles that the stress levels of the participants change significantly between the different sessions of the day, which suggests the induction of physical as well as mental fatigue and related drowsiness.

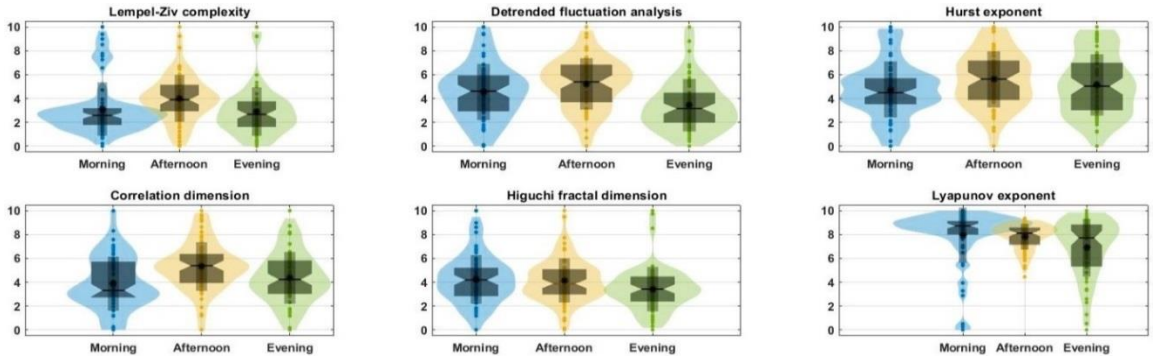

Fig. 15. Violin plots for others complexity parameters of EOGs recorded in morning (MR), afternoon (AN) and evening (EV) sessions.

Table 8. The comparison of complexity parameters of EOGs of morning (MR), afternoon (AN) and evening (EV) in study-II.

Complexiy parameters	Morning Mean ± SEM (95%CI)	Afternoon Mean ± SEM (95%CI)	Evening Mean ± SEM (95%CI)	ANOVA test	Friedman test	Tukey-Kramer Test (post hoc analysis)			ICC
						MR-AN	MR-EV	AN-EV	
Time domain entropy									
ApEn	2.76±0.26 (2.23-3.30)	2.32±0.21 (1.90-2.75)	2.35±0.21 (1.94-2.77)	0.3283 **(NS)**	0.0439	0.0363 **(NS)**	0.2494 **(NS)**	0.6560 **(NS)**	0.91
SampEn	2.93±0.26 (2.40-3.47)	2.45±0.22 (2.01-2.88)	2.58±0.21 (2.16-3.00)	0.3138 **(NS)**	0.0901 **(NS)**	0.0880 **(NS)**	0.8633 **(NS)**	0.2505 **(NS)**	0.90
PeEn	3.11±0.26 (2.59-3.63)	4.23±0.26 (3.71-4.75)	4.60±0.27 (4.05-5.16)	<0.001	<0.0001	<0.0001	<0.0001	<0.0001	0.84
MultiEn	3.93±0.31 (3.30-4.55)	5.36±0.27 (4.83-5.90)	5.23±0.31 (4.60-5.86)	0.0011	<0.001	0.0066	0.0017	0.9155 **(NS)**	0.83
FuzEn	5.17±0.23 (4.69-5.64)	3.44±0.27 (2.90-3.99)	3.96±0.28 (3.40-4.51)	<0.0001	<0.0001	<0.0001	<0.0001	<0.0001	0.85
DispEn	4.02±0.21 (3.58-4.46)	3.88±0.19 (3.49-4.27)	3.07±0.20 (2.66-3.48)	0.0027	<0.0001	0.5334 **(NS)**	<0.0001	<0.0001	0.88
Frequency domain entropy									
TsEn	6.94±0.24 (6.46-7.42)	6.78±0.25 (6.27-7.29)	7.40±0.26 (6.87-7.93)	0.2052 (NS)	<0.001	0.5098 **(NS)**	0.0075	0.0001	0.81
ReEn	3.34±0.24 (2.86-3.83)	3.83±0.25 (3.33-4.32)	3.84±0.25 (3.35-4.34)	0.2700	0.0094	0.5593 **(NS)**	0.0075	0.1180 **(NS)**	0.91
ShEn	3.54±0.24 (3.05-4.03)	3.36±0.25 (2.86-3.86)	2.99±0.26 (2.45-3.52)	0.2905 (NS)	<0.001	0.9464 **(NS)**	0.0045	0.0015	0.83

Others									
LZC	3.11±0.24 (2.61-3.61)	4.00±0.24 (3.56-4.44)	2.89±0.22 (2.44-3.35)	0.0020	<0.0001	<0.0001	0.8820 **(NS)**	<0.0001	0.80
DFA	4.54±0.26 (4.02-5.06)	5.22±0.24 (4.74-5.70)	3.43±0.25 (2.94-3.92)	<0.0001	<0.0001	<0.0001	<0.0001	<0.0001	0.90
HuEx	4.75±0.26 (4.23-5.27)	5.60±0.26 (5.07-6.12)	5.13±0.29 (4.55-5.70)	0.0874 **(NS)**	0.0042	0.0030	0.1118 **(NS)**	0.4059 **(NS)**	0.79
CD	3.88±0.25 (3.37-4.38)	5.31±0.22 (4.86-5.76)	4.36±0.24 (3.88-4.84)	<0.001	<0.0001	<0.0001	0.0558 **(NS)**	0.0558 **(NS)**	0.68
HFD	4.22±0.22 (3.77-4.68)	4.14±0.20 (3.73-4.56)	3.41±0.20 (3.00-3.83)	0.0140 **(NS)**	<0.0001	0.9457 **(NS)**	<0.0001	<0.0001	0.92
LE	7.94±0.25 (7.43-8.46)	6.87±0.24 (6.38-7.36)	6.89±0.27 (6.35-7.43)	0.0042	<0.0001	<0.0001	<0.0001	0.8017 **(NS)**	0.81

To determine the reliability of an experimental procedure, ICCs were measured. ICC varied between 0.68 and 0.91. This indicates that random and systematic errors were recorded [46, 47] and also varies from 9% to 32%. The highest reliability was reported as 0.91 for ApEn.

Table 9. Spearman's rank correlation coefficient (ρ) and Kendall rank correlation coefficient (τ) of complexity parameters of EOGs of morning (MR), afternoon (AN) and evening (EV) discussed in study-II.

Complexity Parameter	**Spearman's rank correlation coefficient *ρ* w.r.t. ApEn, TsEn, ShEn, LZC.**			**Kendall rank correlation coefficient *τ* w.r.t. ApEn, TsEn, ShEn, LZC.**		
	Morning	**Afternoon**	**Evening**	**Morning**	**Afternoon**	**Evening**
ApEn	NA, 0.77, -0.76, 0.54	NA, 0.91, -0.88, 0.52	NA, 0.87, -0.85, 0.64	NA, 0.59, -0.58, 0.39	NA, 0.75, -0.72, 0.39	NA, 0.69, -0.67, 0.46
SampEn	0.85, 0.66, -0.62, 0.27	0.95, 0.87, -0.85, 0.41	0.94, 0.78, -0.75, 0.50	0.69, 0.50, -0.45, 0.16	0.83, 0.70, -0.67, 0.29	0.82, 0.61, -0.59, 0.35
PeEn	0.67, 0.80, -0.83, 0.71	0.72, 0.80, -0.84, 0.67	0.48, 0.83, -0.85, 0.78	0.49, 0.62, -0.66, 0.53	0.52, 0.62, -0.66, 0.50	0.35, 0.65, -0.69, 0.61
MultiEn	0.80, 0.94, -0.95, 0.67	0.86, 0.92 -0.92, 0.61	0.53, 0.94 -0.95, 0.77	0.63, 0.81, -0.81, 0.48	0.68, 0.77 -0.76, 0.45	0.38, 0.82 -0.84, 0.59
FuzEn	-0.46, -0.83, 0.85, -0.56	-0.72, -0.87, 0.91, -0.64	-0.66, -0.91, 0.93, -0.67	-0.33, -0.66, 0.68, -0.40	-0.50, -0.69, 0.74, -0.47	-0.47, -0.74, 0.78, -0.51
DispEn	0.69, 0.43, -0.37, 0.24	0.76, 0.56, -0.51, 0.10	0.79, 0.55, -0.51, 0.27	0.55, 0.30, -0.25, 0.16	0.59, 0.41, -0.36, 0.07	0.63, 0.42, -0.39, 0.20
TsEn	0.77, NA, -0.98, 0.68	0.91, NA, -0.98, 0.68	0.87, NA, -0.99, 0.70	0.59, NA, -0.90, 0.51	0.75, NA, -0.90, 0.52	0.69, NA, -0.92, 0.53
ReEn	0.76, 0.98, -1, 0.71	0.90, 0.99, -1, 0.70	0.86, 0.99, -1, 0.74	0.58, 0.92, -0.97, 0.53	0.75, 0.91, -0.97, 0.53	0.68, 0.92, -0.97, 0.57
ShEn	-0.76, -0.98, NA, -0.74	-0.88, -0.98, NA, -0.71	-0.85, -0.99, NA, -0.74	-0.58, -0.90, NA, -0.56	-0.72, -0.90, NA, -0.55	-0.67, -0.92, NA, -0.58
LZC	0.54, 0.68, -0.74, NA	0.52, 0.68, -0.71, NA	0.64, 0.70, -0.74, NA	0.39, 0.51 -0.56, NA	0.39, 0.52, -0.55, NA	0.46, 0.53, -0.58, NA
DFA	-0.08, -0.12, 0.14, -0.41	0.01, -0.03, 0.03, -0.32	0.06, -0.02, 0.06, -0.26	-0.08, -0.09, 0.10, -0.27	0, -0.03, 0.03, -0.22	0.05, -0.02, 0.05, -0.18
HuEx	0.53, 0.52, -0.55, 0.43	0.42, 0.44, -0.51, 0.47	0.48, 0.58, -0.57, 0.46	0.37, 0.36, -0.38, 0.31	0.30, 0.33, -0.37, 0.33	0.36, 0.42, -0.41, 0.34
CD	0.72, 0.65, -0.66, 0.37	0.60, 0.55, -0.49, 0.19	0.80, 0.75, -0.75, 0.47	0.52, 0.47, -0.47, 0.22	0.42, 0.39, -0.34, 0.13	0.60, 0.56, -0.56, 0.31
HFD	0.63, 0.52, -0.56, 0.73	0.57, 0.58, -0.59, 0.75	0.62, 0.60, -0.61, 0.74	0.45, 0.37, -0.40, 0.50	0.42, 0.43, -0.44, 0.58	0.44, 0.46, -0.47, 0.58
LE	-0.52, -0.74, 0.77, -0.72	-0.58, -0.71, 0.75, -0.67	-0.60, -0.68, 0.70, -0.73	-0.37, -0.56, 0.59, -0.56	-0.41, -0.52, 0.56, -0.50	-0.46, -0.51, 0.53, -0.56

The non-parametric spearman's rank correlation coefficient (ρ) and Kendall rank correlation coefficient (τ) are used to compare the interaction between all the complexity parameters with time domain (ApEn), frequency domain (TsEn and ShEn) and others (LZC) complexity parameters are shown in Table 9. Excellent negative correlation (Spearman's rank and Kendall rank) was found as ρ=-1 and τ=-0.97 between ReEn and ShEn irrespective of sessions of the day. Negative correlations were obtained due to inverse relation between two complexity parameters [49]. Excellent positive correlation (0.98, 0.99, 0.99 for spearman's rank and 0.92, 0.91, 0.92 for Kendall rank) was also obtained between ReEn and TsEn.

4. Experimental Limitation

The present investigation was conducted on male and female individuals who self-reported as being mentally and physically healthy, solely relying on the information provided by subjects. However, we cannot promise the accuracy or completeness of the self-reported history. As the subjects of the research were of a homogeneous age group, it is not possible to extrapolate any findings or inferences to other age demographics, such as children or older adults. As the data for all three sessions of a subject were collected on a same day, this study is unable to ascertain the extent of

variation across multiple days. Several natural factors, such as inadequate sleep, prolonged mental or physical exertion, extended stress or anxiety, mood, alertness, lifestyle, and the menstrual cycle phases in women, are challenging to regulate in studies of this nature, as they can contribute to fatigue.

5. Conclusion

The main aim is to investigate on fatigue and drowsiness of the research scholars of National Institute of Technology Durgapur, India, due to cognitive loading throughout the different sessions of the day. In this present study the variation of complexity parameters is experimentally and statistically analyzed. Study-I shows the variation of complexity parameters for four patterns of cue movement- for morning and evening and non-parametric Wilcoxon-test was performed to reinforce the experimental study. Study-II depicts the variation of complexity parameters in three different sessions viz. morning, afternoon and evening. Non parametric Friedman test was employed to find the statistical variations among these three sessions. Whenever significant difference is investigated among group measures, Tukey-Kramer post hoc analysis was performed. In study-I, the Wilcoxon test findings show that almost all of the complexity parameters of EOGs for RCW, with the exception of SampEn and HuEx, clearly differ between a morning and evening session with a $p<0.05$. With the exception of ApEn and TsEn, practically all complexity parameters with $p<0.05$ in the Wilcoxon test for RAC support the substantial difference between the morning session and evening session. The Wilcoxon test further supports ApEn, SampEn, PeEn, FuzEn, DispEn, TsEn, ReEn, ShEn, LZC, DFA, HuEx and LE are showing significant differences between morning and evening session at 5% significance level for TCW and ApEn, MultiEn, FuzEn, DispEn, TsEn, ReEn, ShEn, LZC, DFA, CD and LE are showing prominent differences between the two sessions with threshold level $p<0.05$ for TAC. The Bland-Altman plot also substantiate the difference in entropies and complexity parameters between morning and evening sessions and the most of complexity indices are not identical for all the four cue movements due to induced fatigue into muscle. In study-II, the Friedman test results evident that all the time domain entropies except SampEn, all the frequency domain entropies and all the others complexity parameters are showing a significant difference for $p < 0.05$ among morning, afternoon and evening sessions. In order to assess the changes between morning-afternoon, morning-evening and afternoon-evening, Tukey-Kramer test was performed. Further ApEn, TsEn, ShEn, LZC as covariables, non-parametric Spearman's rank and Kendall rank tests were conducted. ReEn has the highest ($\rho=0.99$, $\tau=0.92$) positive association with TsEn and ($\rho=-1$, $\tau=-0.97$) negative association with ShEn. Therefore, it can be concluded that the, correlation coefficients do not alter with the session of the day, whereas the complexity parameters are affected by sessions of acquisition i.e., morning, afternoon and evening. These results help future fatigue studies apply to more extensive areas and people of diverse ages. Future research will attempt to apply this statistical approach or similar computational techniques to cluster and classify data to identify various fatigue levels and provide the person in question with a real-time alarm. In addition to cognitive activities, other factors like inadequate sleep, drugs, and additional physical or mental stress may also be considered.

Conflict of Interest

The authors declare there is no conflict of interest for this study.

References

[1] Global status report on road safety 2018: summary. Geneva: World Health Organization; summary. Geneva: World Health Organization;

[2] F.W. Wang, Q. Xu, R.R. Fu, "Study on the effect of man-machine response mode to relieve driving fatigue based on EEG and EOG." Sensors (2019).

[3] Y. Liu, A.G. Wheaton, D.P. Chapman, T.J, Cunningham, H. Lu, J.B. Croft, "Prevalence of Healthy Sleep Duration among Adults — United States, 2014," MMWR Morb Mortal Wkly Rep, vol.65, pp. 137–141, 2016.

[4] G. Yang, Y. Lin, and P. Bhattacharya, "A driver fatigue recognition model based on information fusion and dynamic Bayesian network. Inf. Sci. vol. 180, no. 10, pp. 1942–1954, 2010.

[5] P. Thiffault and J. Bergeron, "Monotony of road environment and driver fatigue: A simulator study," Accident Anal. Prevention, vol. 35, no. 3, pp. 381–391, 2003.

[6] C. Varghese and U. Shankar, "Passenger vehicle occupant fatalities by day and night-a contrast," Nat. Highway Traffic Safety Admin., vol. 51, no. 4, p. 443, 2008.

[7] S. Nordbakke, F. Sagberg, "Sleepy at the wheel: Knowledge, symptoms and behaviour among car drivers," Transportation Research Part F: Traffic Psychology and Behaviour, vol. 10, no. 1, pp 1-10, 2007.

[8] W. Gottlieb, L. Galley, R. Schleicher, N. Galley, and J. Churan, "EEG and ocular parameters while driving in a simulation study," Tech. Rep., 2004.

[9] R.N. Khushaba, S. Kodagoda, S. Lal, G. Dissanayake, "Uncorrelated fuzzy neighbourhood preserving analysis-based feature projection for driver drowsiness recognition," Fuzzy Sets Syst, vol. 221, pp. 90–111, 2013.

[10] W.Z. Kong, W.C. Lin, B. Fabio, S.Q. Hu, B. Gianluca, "Investigating driver fatigue versus alertness using the granger causality network," Sensors vol. 15, no. 8, pp. 19181–19198, 2015.

[11] Z.K. Gao, X.M. Wang, Y.X. Yang, C.X. Mu, Q. Cai, W.D. Dang, S.Y. Zuo, "EEG-based spatio-temporal convolutional neural

network for driver fatigue evaluation," IEEE Trans. Neural Netw. Learning Syst. Vol. 30, no. 9, pp. 2755–2763, 2019.
[12] C. Zhang, H. Wang and R. Fu, "Automated Detection of Driver Fatigue Based on Entropy and Complexity Measures," IEEE Transactions on Intelligent Transportation Systems, vol. 15, no. 1, pp. 168-177, 2014.
[13] M. Lin, H. Liang, K. Lin and Y. Hwang, "Electromyographical assessment on muscular fatigue—an elaboration upon repetitive typing activity," Journal of Electromyography and Kinesiology, vol. 14, no. 6, pp. 661-669, 2004.
[14] S.Y. Hu, G.T. Zheng, "Driver drowsiness detection with eyelid related parameters by Support Vector Machine," Expert Syst. Appl., vol. 36, no. 4, pp. 7651–7658, 2009.
[15] A. K. Kokonozi, E. M. Michail, I. C. Chouvarda and N. M. Maglaveras, "A study of heart rate and brain system complexity and their interaction in sleep-deprived subjects," Computers in Cardiology, pp. 969-971, 2008.
[16] S. J. Jung, H. S. Shin and W. Y. Chung, "Driver fatigue and drowsiness monitoring system with embedded electrocardiogram sensor on steering wheel," IET Intelligent Transport Systems, vol. 8, no. 1, pp. 43–50, 2014.
[17] S. Kar and A. Routray, "Effect of Sleep Deprivation on Functional Connectivity of EEG Channels," IEEE Transactions on Systems, Man, and Cybernetics: Systems, vol. 43, no. 3, pp. 666-672, 2013.
[18] J.N. Côté, D. Raymond, P.A. Mathieu, A.G. Feldman, M.F. Levin, "Differences in multijoint kinematic patterns of repetitive hammering in healthy, fatigued and shoulderinjured individuals," Clin Biomech (Bristol, Avon), vol. 20, no. 6, pp. 581-90, 2005.
[19] H. Iridiastadi, M.A. Nussbaum, "Muscle fatigue and endurance during repetitive intermittent static efforts: development of prediction models," Ergonomics, vol. 49, vol. 4, pp. 344-60, 2006.
[20] K. Bylykbashi, E. Qafzezi, M. Ikeda, K. Matsuo, L. Barolli, "Fuzzy-based Driver Monitoring System (FDMS): Implementation of two intelligent FDMSs and a testbed for safe driving in VANETs," Future Generation Computer Systems, vol. 105, pp 665-674, 2020.
[21] Y. Wang, R. Huang and L. Guo, "Eye gaze pattern analysis for fatigue detection based on GP-BCNN with ESM. Pattern Recognition Letters, vol. 123, pp. 61-74, 2019.
[22] J. Li, H. Li, W. Umer, H. Wang, X. Xing, S. Zhao and J. Hou, "Identification and classification of construction equipment operators' mental fatigue using wearable eye-tracking technology," Automation in Construction, vol. 109, 103000, 2020.
[23] "World Medical Association," World Medical Association Declaration of Helsinki: Ethical Principles for Medical Research Involving Human Subjects. JAMA. Vol. 310 no. 20, pp:2191–2194, 2013.
[24] Ashis Kumar Das, Prashant Kumar, Suman Halder, Anwesha Banerjee, D.N. Tibarewala, "A Laboratory Based Experimental Evaluation of Ocular Parameters as Fatigue and Drowsiness Measures," Procedia Computer Science, vol. 167, pp. 2051-2059, 2020.
[25] S. Datta, A. Banerjee, M. Pal, A. Konar, D. N. Tibarewala and R. Janarthanan, "Blink recognition to detect the possibility of eye dystonia based on electrooculogram analysis," Proceedings of the 2014 International Conference on Control, Instrumentation, Energy and Communication (CIEC), Calcutta, pp. 186-190.
[26] Anwesha Banerjee, Monalisa Pal, Shreyasi Datta, D.N. Tibarewala, Amit Konar, Eye movement sequence analysis using electrooculogram to assist autistic children, Biomedical Signal Processing and Control, vol 14, pp. 134-140, 2014.
[27] C. E. Shannon, "A mathematical theory of communication," The Bell System Technical Journal, vol. 27, no. 3, pp. 379-423, 1948.
[28] Steve Pincus , "Approximate entropy (ApEn) as a complexity measure", Chaos 5, pp. 110-117, 1995.
[29] Joanna Olbrys, Elzbieta Majewska, "Approximate entropy and sample entropy algorithms in financial time series analyses," Procedia Computer Science, vol. 207, pp. 255-264, 2022.
[30] J.M. Yentes, N. Hunt, K.K. Schmid et al., "The Appropriate Use of Approximate Entropy and Sample Entropy with Short Data Sets," Ann Biomed Eng, vol.41, pp. 349–365, 2013.
[31] J.S. Richman, D.E. Lake, J.R. Moorman, "Sample entropy," Methods Enzymol, Vol. 384, pp:172-84, 2004.
[32] C. Bandt, B. Pompe, "Permutation Entropy: A Natural Complexity Measure for Time Series," Phys. Rev. Lett., vol. 88, 174102, 2002.
[33] Jinyang Li, Pengjian Shang, Xuezheng Zhang, "Financial time series analysis based on fractional and multiscale permutation entropy," Communications in Nonlinear Science and Numerical Simulation, vol. 78, 2019.
[34] M. Costa, A.L. Goldberger, C. K. Peng, "Multiscale entropy analysis of complex physiologic time series," Phys. Rev. Lett., vol. 89, 068102, 2002.
[35] W. Chen, Z. Wang, H. Xie and W. Yu, "Characterization of Surface EMG Signal Based on Fuzzy Entropy," IEEE Transactions on Neural Systems and Rehabilitation Engineering, vol. 15, no. 2, pp. 266-272, 2007.
[36] M. Rostaghi and H. Azami, "Dispersion Entropy: A Measure for Time-Series Analysis," IEEE Signal Processing Letters, vol. 23, no. 5, pp. 610-614, 2016.
[37] Tsallis, Constantino, "Generalized entropy-based criterion for consistent testing. Phys. Rev. E Stat. Phys. Plasmas Fluids Relat.Interdiscip. Top., vol. 58, pp. 1442–1445, 1998.
[38] Mehran Azimbagirad, Luiz Otavio Murta Junior, "Tsallis generalized entropy for Gaussian mixture model parameter estimation on brain segmentation application," Neuroscience Informatics, vol. 1, no. 1–2, 2021.
[39] R.K. Pathria, Beale, Paul, "Shannon entropy," Statistical Mechanics (Third ed.). Academic Press, p. 51, 2011.
[40] A. Lempel and J. Ziv, "On the Complexity of Finite Sequences," IEEE Transactions on Information Theory, vol. 22, no. 1, pp. 75-81, 1976.
[41] C.K. Peng, S.V. Buldyrev, S. Havlin, M. Simons, H.E. Stanley, A.L. Goldberger, "Mosaic organization of DNA nucleotides," Phys Rev E Stat Phys Plasmas Fluids Relat Interdiscip Topics, vol. 49, no. 2, pp. 1685-9, 1994.
[42] B. Qian and K.M. Rasheed, "Hurst Exponent And Financial Market Predictability," 2005
[43] N. Sriraam, "Correlation dimension based lossless compression of EEG signals," Biomedical Signal Processing and Control, vol. 7, no. 4, pp. 379-388, 2012.
[44] T. Higuchi, "Approach to an irregular time series on the basis of the fractal theory," Physica D: Nonlinear Phenomena, vol. 31, no. 2, pp. 277-283, 1988.
[45] J. Jeong, J.H. Chae, S.Y. Kim, S.H. Han, "Nonlinear dynamic analysis of the EEG in patients with Alzheimer's disease and vascular dementia," J Clin Neurophysiol, vol. 18, no. 1, pp:58-67, 2001.

[46] D.G. Altman, and J.M. Bland, "Measurement in Medicine: The Analysis of Method Comparison Studies," The Statistician, vol. 32, pp. 307-317, 1983.
[47] Rafdzah Zaki, Awang Bulgiba, Noor Azina Ismail, "Testing the agreement of medical instruments: Overestimation of bias in the Bland–Altman analysis," Preventive Medicine, vol. 57, Supplement, pp. S80-S82, 2013.
[48] D. Liljequist, B. Elfving and K.S. Roaldsen, "Intraclass correlation – A discussion and demonstration of basic features," PLoS ONE, vol. 14, no. 7, 2019.
[49] C. Langner, E. Svensson and S. Harvey, "Flexibility analysis of chemical processes considering dependencies between uncertain parameters," Computer Aided Chemical Engineering, vol. 50, pp. 1105-1110, 2021.

Authors' Profiles

Ashis Kumar Das completed his B.E. (Electrical & Electronics Engineering, 2004) and M.Tech. (Industrial Electrical System, 2006) from University of North Bengal, West Bengal and National Institute of Technology Durgapur, West Bengal, respectively. He is currently associated with Faculty of Technology, UBKV, Cooch Behar, India from 2007 and pursuing his PhD at Electrical Engineering Department, National Institute of Technology Durgapur, India. His special field of interest includes biomedical signal processing, biomedical instrumentation, signal processing, artificial intelligence.

Prashant Kumar completed his B.Tech (Electrical Engineering, 2013) and M.E. (Electrical, 2016) from Maulana Abul Kalam Azad University of Technology, West Bengal and National Institute of Technical Teachers Training and Research, Chandigarh, respectively. He is currently pursuing his PhD under the supervision of Dr. Suman Halder at Electrical Engineering Department, National Institute of Technology Durgapur, India.

Suman Halder completed his BE (Electrical, 2001), ME (Electrical, 2004) and PhD (Engineering, 2009) from Jadavpur University, respectively. He is associated with NIT Durgapur, India from 2014 and currently working on biomedical instrumentation and signal analysis.

Santanu Metia received the B.E. degree in electrical engineering from the Jalpaiguri Government Engineering College, India, in 1997, the M.S. degree in electrical engineering from the Indian Institute of Technology Kharagpur, India, in 2002, and the Ph.D. degree from the University of Technology Sydney, Australia, in 2016. He is currently a Research Associate with the University of Technology Sydney. He conducted research on mobile robotics at Swiss Federal Institute of Technology Lausanne, Switzerland. He involved in Tyristor Controlled Series Compensator project at Indian Institute of Technology, Kanpur, India. His research interests include Kalman filtering, fractional systems, indoor air quality modeling, climate change, and air quality modeling, biomedical signal processing.

How to cite this paper: Ashis Kumar Das, Prashant Kumar, Suman Halder, Santanu Metia, "A Statistical Approach for Investigation and Comparison of Fatigue and Drowsiness based on Complexity Parameters of EOGs", International Journal of Image, Graphics and Signal Processing(IJIGSP), Vol.15, No.5, pp. 39-59, 2023. DOI:10.5815/ijigsp.2023.05.04